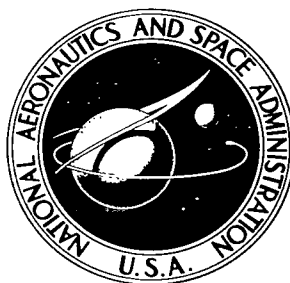


NASA TECHNICAL NOTE



NASA TN D-3839

e.1

NASA TN D-3839

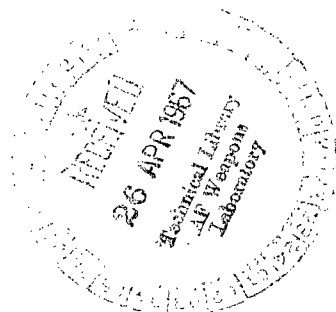
LOAN COPY: RETURN
AFWL (WLIL-2)
KIRTLAND AFB, N M



APPLICATION OF A DOUBLE LINEAR DAMAGE RULE TO CUMULATIVE FATIGUE

by S. S. Manson, J. C. Freche, and C. R. Ensign

*Lewis Research Center
Cleveland, Ohio*





APPLICATION OF A DOUBLE LINEAR DAMAGE RULE TO
CUMULATIVE FATIGUE

By S. S. Manson, J. C. Freche, and C. R. Ensign

Lewis Research Center
Cleveland, Ohio

NATIONAL AERONAUTICS AND SPACE ADMINISTRATION

For sale by the Clearinghouse for Federal Scientific and Technical Information
Springfield, Virginia 22151 - CFSTI price \$3.00

APPLICATION OF A DOUBLE LINEAR DAMAGE RULE TO CUMULATIVE FATIGUE*

by S. S. Manson, J. C. Freche, and C. R. Ensign

Lewis Research Center

SUMMARY

The validity of a previously proposed method of predicting cumulative fatigue damage in smooth 1/4-inch-diameter specimens based on the concept of a double linear damage rule was investigated. This method included simplified formulas for determining the crack initiation and the propagation stages and indicated that each of these stages could be represented by a linear damage rule. The present study provides a critical evaluation of the earlier proposal, further illuminates the principles underlying cumulative fatigue damage, and suggests a modification of the original proposal.

The data were obtained in two-stress-level tests with maraging and SAE 4130 steels in rotating bending. Also, two-strain-level tests were conducted in axial reversed strain cycling with a maraging steel. The investigation showed that in most cases the double linear damage rule when used in conjunction with originally proposed equations for determining crack initiation and propagation predicted fatigue life with equal or greater accuracy than the conventional linear damage rule. An alternative viewpoint of the double linear damage rule is suggested. This viewpoint requires that a limited number of simple two-stress-level tests be run to establish effective fatigue curves for what may be defined as Phases I and II of the fatigue process. These fatigue curves may then be used in the analysis of any spectrum of loads involving as loading extremes the two stresses used for their determination. Only limited verification of the new method has been obtained to date, and it must presently be limited to the study of smooth, 1/4-inch-diameter specimens. However, it may be considered as a first step in the direction of eventually predicting the effect of a complex loading history on the life of more complex geometrical shapes.

INTRODUCTION

The subject of cumulative fatigue damage is extremely complex, and various theories have been proposed (refs. 1 to 10) to predict fatigue life in advance of service. The most widely known and used procedure is the linear damage rule commonly called the Miner rule (ref. 7). The linear damage rule, which indicates that a summation of cycle ratios is equal to unity, is not completely accurate; however, because of its simplicity and

* Presented at Symposium on Crack Propagation sponsored by the American Society for Testing Materials, Atlantic City, New Jersey, June 26 to July 1, 1966.

because of its agreement with experimental data for certain cases it is frequently used in design. If a new method is to replace the linear damage rule in practical design, much of the simplicity of the linear damage rule must be retained. The double linear damage rule, considered herein, retains much of this simplicity and at the same time attempts to overcome some of the limitations inherent in the conventional linear rule.

One of the limitations of the linear damage rule is that it does not consider the effect of order of loading. For example, in a two-stress-level fatigue test in which a high load is followed by a low load, the cycle ratio summation is less than 1, whereas a low load followed by a high load produces a cycle ratio summation greater than 1. The effect of residual stress is also not properly accounted for by the conventional linear damage rule, nor does it consider cycle ratios applied below the initial fatigue limit of the material. Since prior loading can reduce the fatigue limit, cycle ratios of stresses applied below the initial fatigue limit should be accounted for (ref. 10). In addition, coxing effects present in some strain-aging materials (ref. 11) in which the appropriate sequence of loading may progressively raise the fatigue limit are not accounted for by the linear damage rule. Various methods have been proposed as alternatives to the linear damage rule. None overcomes all the deficiencies, and many introduce additional complexities that either preclude or make their use extremely difficult in practical design problems.

The possibility of improving the predictions of a linear damage rule by breaking it up into two phases, a linear damage rule for crack initiation and a linear damage rule for crack propagation, was first suggested by Grover in reference 12. Neither a rational basis for this approach was indicated nor were definite expressions provided for separating the two phases. These aspects were considered in greater detail in reference 13. Total life was considered as consisting of two important phases, one for initiating a crack and one for propagating a crack, and a linear damage rule was applied to each of these phases. This double linear damage rule was intended to correct the deficiencies associated with order of loading; the other limitations previously cited were not directly considered. Simplified formulas derived from limited data for determining the crack initiation and the propagation stages were tentatively presented.

The present study was conducted to provide a critical evaluation of the proposal of reference 13, specifically, the analytical expressions for separating the two phases. Additional data were obtained in two-stress-level tests in rotating bending and two-strain-level tests in axial reversed strain cycling. The materials investigated were maraging and SAE 4130 steels. Fatigue life predictions by the double linear damage rule and the conventional linear damage rule are compared with experimental data. In addition, instead of using the analytical expression given in reference 13 to represent the crack propagation stage in the application of the double linear damage rule as originally proposed, a more generalized expression is suggested that involves the separation of the fatigue process into two experimentally determined phases. These phases are not necessarily the physical processes of crack initiation and propagation.

CONCEPT OF THE DOUBLE LINEAR DAMAGE RULE

Analytical Application

In reference 13 it is proposed that the crack propagation period $(\Delta N)_f$ and crack initiation N_o can both be expressed in terms of total fatigue life N_f by the following equations:

$$(\Delta N)_f = PN_f^{0.6} \quad (1)$$

and

$$N_o = N_f - (\Delta N)_f = N_f - PN_f^{0.6} \quad (2)$$

where the coefficient $P = 14$. The experimental basis for the selection of this value of coefficient is given in references 13 and 14 and is also further described subsequently herein.

The equations expressing cumulative fatigue damage in terms of the double linear damage rule, as proposed in reference 13, are as follows:

For the crack initiation phase,

$$\sum \frac{n}{N_o} = 1 \quad \begin{array}{l} \text{(when } N_f > 730 \text{ cycles, } N_o = N_f - 14 N_f^{0.6} \\ \text{when } N_f < 730 \text{ cycles, } N_o \approx 0) \end{array} \quad (3)$$

If any part of the loading spectrum includes a condition where $N_f < 730$ cycles, an effective crack is presumed to initiate upon application of that first loading cycle.

For the crack propagation phase,

$$\sum \frac{n}{(\Delta N)_f} = 1 \quad \begin{array}{l} \text{(when } N_f > 730 \text{ cycles, } (\Delta N)_f = 14 N_f^{0.6} \\ \text{when } N_f < 730 \text{ cycles, } (\Delta N)_f = N_f) \end{array} \quad (4)$$

where

N_o cyclic life to initiate effective crack at particular strain or stress level

$(\Delta N)_f$ cyclic life to propagate crack from initiation to failure at particular strain or stress level

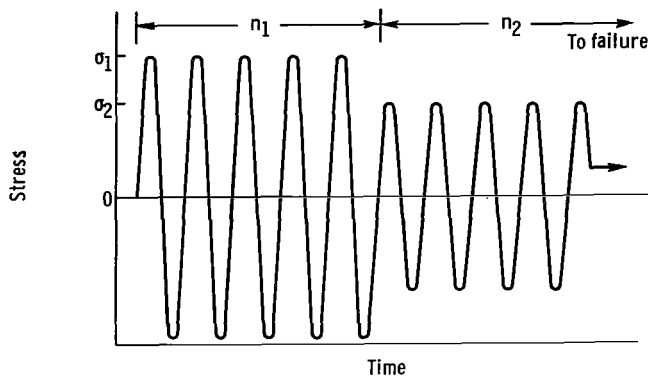
N_f cyclic life to failure of specimen

n number of cycles applied at particular strain or stress level

An example of the manner of applying these equations for simple two-stress-level loading is given in appendix A. Further discussion of the equation relating crack initiation and propagation to total fatigue life is presented in reference 14. It should be emphasized that these equations were derived on the basis of data obtained with 1/4-inch-diameter (6.35-mm) specimens of notch ductile materials and have thus far been shown to be valid only for this size specimen (ref. 14). Of course, most materials would be notch ductile for such a small specimen size. This aspect is discussed more fully in reference 13.

By comparison, the conventional linear damage rule is expressed as

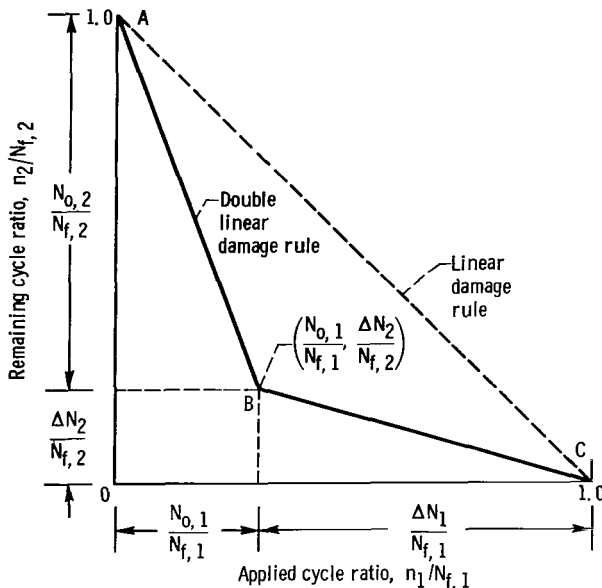
$$\sum \frac{n}{N_f} = 1 \quad (5)$$



(a) Schematic drawing of loading pattern.

Equation (5) states that a single summation of cycle ratios applied at different stress or strain levels is equal to 1.

Graphical Representation of Double Linear Damage Rule Applied to Two-Stress-Level Fatigue Test



(b) Interpretation of fatigue damage by linear damage rules.

Figure 1. - Two-stress-level fatigue tests.

Figure 1 illustrates the graphical representation of the double linear damage rule plotted in terms of the remaining cycle ratio $n_2/N_{f,2}$ at a second stress level against the cycle ratio $n_1/N_{f,1}$ applied at an initial stress level. Also shown is a dashed 45° line, which represents the conventional linear damage rule. The figure is illustrative of the case in which the prestress condition is the high stress, and this condition is followed by operation to failure at a lower stress. The position of lines AB and BC would be located on the other

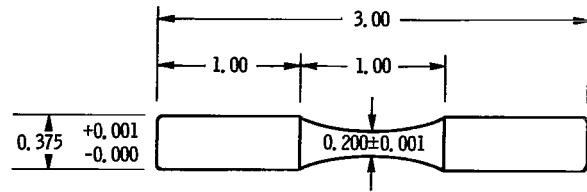
side of the 45° line for the condition of low prestress followed by operation to failure at a high stress. According to the double linear damage rule, if the cycle ratio applied $n_1/N_{f,1}$ is less than that required to initiate an effective crack at a particular stress level, then the remaining predicted cyclic life ratio $n_2/N_{f,2}$ would be along AB (fig. 1). The linearity of AB is implicit in the assumption of a linear damage rule for crack initiation. Point B represents the cycle ratio applied at the first stress level, which is sufficient to initiate an effective crack, so that upon changing to the second stress level the remaining cycle ratio at that stress level is exactly equal to the total propagation stage. The coordinates of this point are designated as $N_{o,1}/N_{f,1}$ and $\Delta N_2/N_{f,2}$. Beyond this initial cycle ratio $N_{o,1}/N_{f,1}$, the first applied cycle ratio is more than that required to initiate an effective crack, and the crack propagation phase is entered. This phase is represented by the line BC, which is also straight and reflects the second assumed linear relation. The remaining cyclic life ratio then is along line BC. Thus, in two-step tests in which a single stress level was applied for a given cycle ratio and the remainder of the life taken up at a second stress level, two straight lines positioned as shown would be expected. It should also be emphasized that point B is significant since it permits determination of both the effective crack initiation and the propagation periods for both stress levels used in the test.

A final point should be made with respect to the graphical application of the double linear damage rule. Since lines AB and BC are straight and since points A and C are fixed, ideally only two tests are required to establish the positions of these lines and, consequently, the point B. The only requirement for selecting these tests is that in one test the cycle ratio applied at the initial stress level should be relatively large, and for the other test it should be relatively small, in order to ensure that the remaining cycle ratios $n_2/N_{f,2}$ do not both fall on the same straight line, either AB or BC. The significance of obtaining point B in this simple fashion is apparent in the illustrative examples of appendixes B and C.

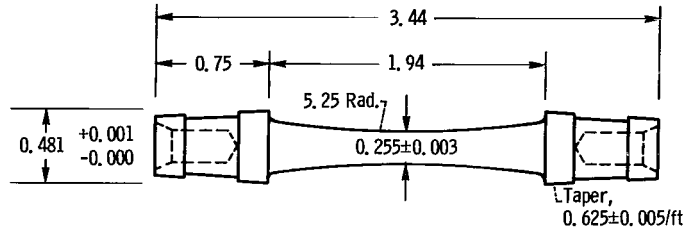
EXPERIMENTAL PROCEDURE

Materials

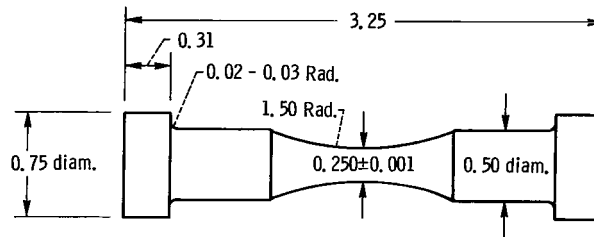
Two steels, SAE 4130 and an 18-percent nickel maraging steel (consumable electrode vacuum melted), were investigated. Their compositions, heat treatments, and hardnesses are listed in table I and their tensile properties in table II. Two different types of test specimens were used to accommodate the R. R. Moore and Krouse rotating bending test machines. A third type of specimen was used for axial strain cycling tests. All three specimen types are shown in figure 2. The 4130 steel test specimens were



(a) Krouse rotating bending specimen.



(b) R. R. Moore rotating bending specimen.



(c) Axial fatigue test specimen.

Figure 2. - Fatigue specimens. (Dimensions are in inches. Conversion factor, 1 in. = 2.54 cm.)

machined after heat treatment. The maraging steel specimens were machined prior to aging and after aging were finish ground to remove the final 0.015 inch (0.38 mm) from the test section. In addition, all rotating bending specimens were machine polished with abrasive cloth of three grit sizes (320, 400, and 500). After final polishing the specimens were subjected to a microscopic examination at a magnification of 20.

Tests

Specimens were subjected to rotating bending in modified R. R. Moore and Krouse (200 in.-lb capacity) rotating-beam fatigue machines and to axial reversed strain cycling in hydraulically actuated axial fatigue machines. In the rotating bending tests, a rotational speed of 5000 rpm (83.3 Hz) was employed at the lower stress levels. In order to avoid the detrimental effect of severe heat accumulation due to hysteresis, rotational speeds as low as 100 rpm (1.67 Hz) were employed at the higher stresses, and jets of

cooling air were directed at the specimens. A specimen runout no greater than 0.001 inch (0.025 mm) full indicator reading was permitted upon installation into the fatigue machines. Additional details regarding the rotating bending test procedure are given in references 9 and 10. Axial fatigue tests were run at 20 cycles per minute (0.33 Hz). Details of the test procedure are given in reference 15.

The fatigue curves for each material were obtained by fairing the best visual-fit curves through the median data points obtained at each stress or strain range level. In conducting the investigation, specimens were prestressed at a single stress (in rotating bending tests) to the desired percentage of material life as determined from the fatigue curves of the original material and to a single strain range (axial fatigue tests) as determined from strain-range - life curves of the original material. The specimens were then run to failure at various stress (or strain range) levels. The specific test conditions are indicated on the figures that present the data and in tables III to VI. There was one exception to this procedure. For one test series, an alternating two-stress-level test was employed in rotating bending. This test is described in appendix C and table VII.

RESULTS AND DISCUSSION

Comparison of Experimental and Predicted Fatigue Life by Originally Proposed Double Linear Damage Rule and Conventional Linear Damage Rule

Figure 3 shows the results reported previously in reference 13 for maraging steel,

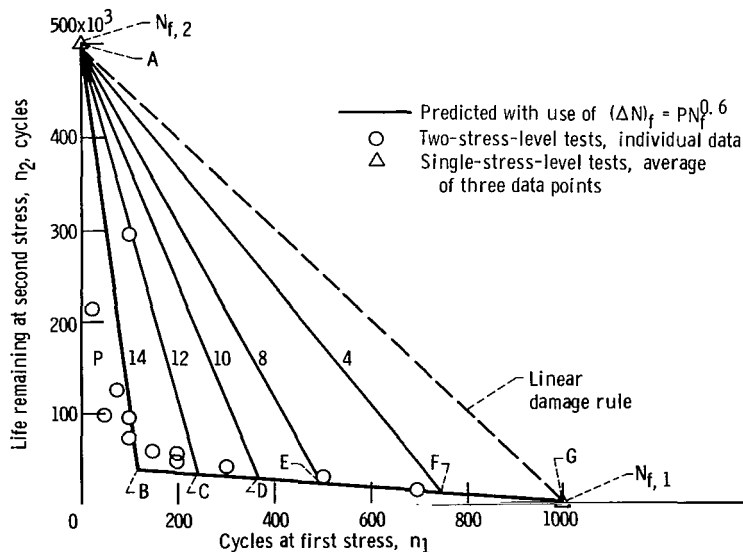
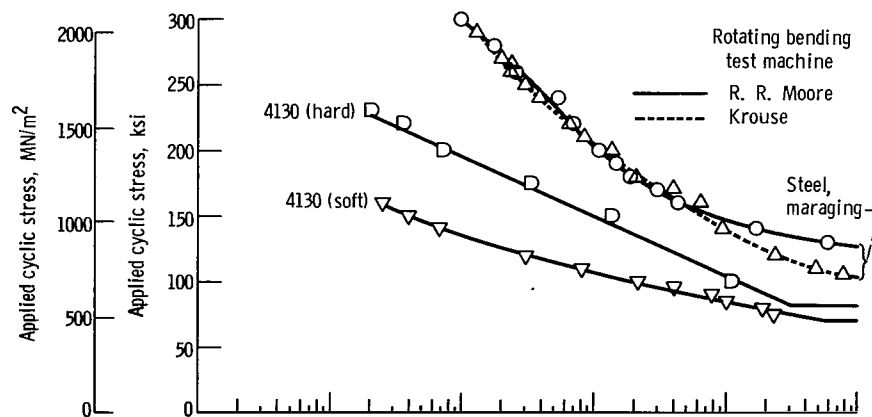


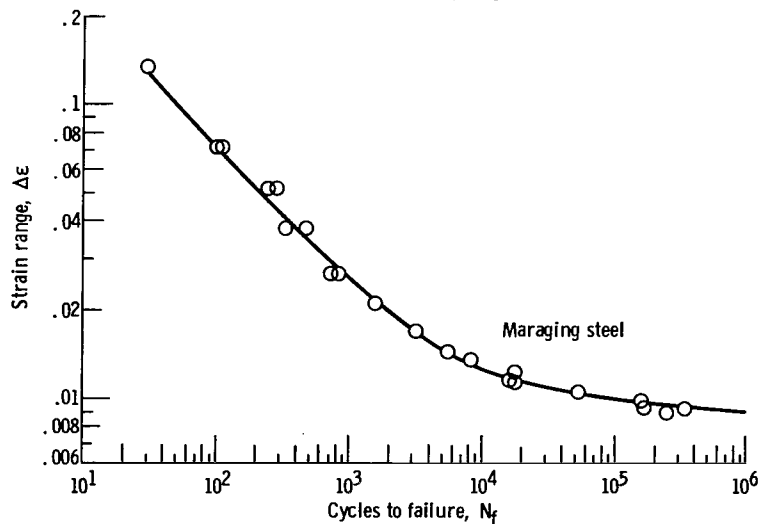
Figure 3. - Two-stress-level rotating bending fatigue tests for determination of coefficient in expression for crack propagation. Material, maraging steel.

which were obtained from rotating bending tests. The stress levels were so chosen that life at the initial stress was approximately 1000 cycles and at the second stress 500 000 cycles. Experimental data are shown by the circles. The solid lines represent predicted behavior by the double linear damage rule with the use of different values of the coefficient in equation (1). For a value of coefficient equal to 14, the predicted behavior was represented by the line ABG; for a coefficient of 12, it was ACG, etc. If a linear damage rule applied for the total life values, the behavior would be that shown by the dashed line AG. A reasonable agreement with the experimental data was obtained for a coefficient of 14. Since these data represent only one material and one combination of high and low stress, equation (1) was only tentatively proposed (ref. 13) as being representative of cumulative fatigue damage behavior.

In extending this approach, many additional tests were conducted with the same and



(a) Rotating bending fatigue life.



(b) Axial fatigue life of maraging steel.

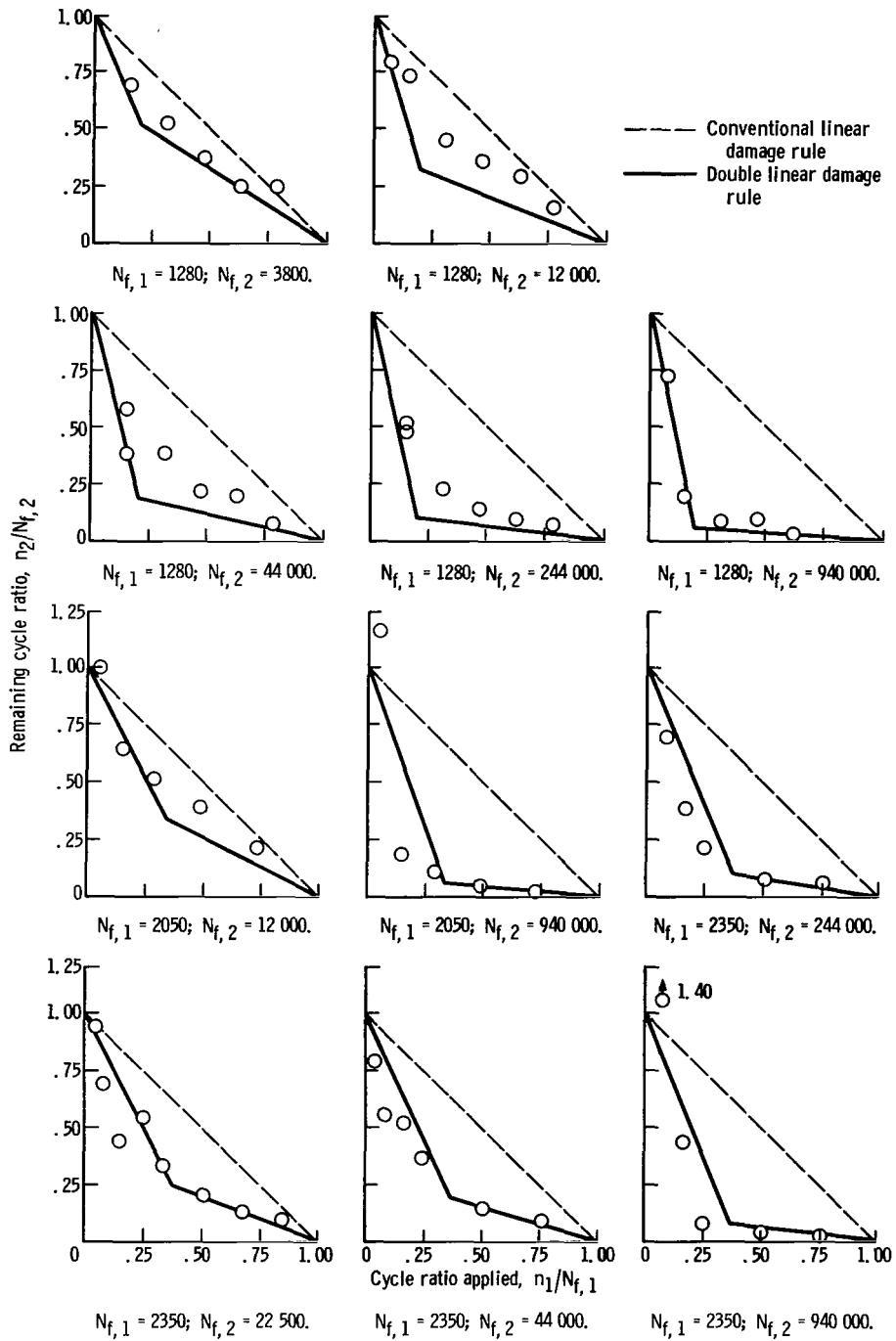
Figure 4. - Fatigue curves for materials investigated.

with other materials in rotating bending and axial reversed strain cycling. Figure 4 shows the fatigue curves of these materials, maraging steel and hard and soft SAE 4130 steel. Since both Krouse and R. R. Moore machines were used for the maraging steel tests, the fatigue curves obtained with each machine are shown (fig. 4(a)). The curves are nearly coincident. Figure 4(b) shows the fatigue curve for maraging steel obtained in axial reversed strain cycling.

Predictions of fatigue behavior by the double linear damage rule (with the expression $14 N_f^{0.6}$ representing the crack-propagation stage) and by the conventional linear damage rule are compared with experimental data in figures 5 and 6. Different combinations of load that correspond to different life levels were chosen. Figure 5(a) presents the results from rotating bending tests for maraging steel designed to give relatively low fatigue lives of 1280, 2050, and 2350 cycles at the initial stress level. The loads at the second stress level were chosen to give lives up to 940 000 cycles. Generally, the greater the difference between the initial and the final life level (i. e. , initial and final stress applied), the greater the deviation between the experimental data and the predicted behavior by the conventional linear damage rule shown by the 45° dashed line; also, the steeper is the first (corresponding to line AB, fig. 1, p. 4) of the two solid lines, which predicts fatigue behavior by the double linear damage rule. Agreement between predicted fatigue behavior by the double linear damage rule and experimental data is good for these test conditions. This agreement might be expected since the higher stress level as well as some of the lower stress levels are generally of the same order as those selected originally for determining equation (1) for this same material in reference 13.

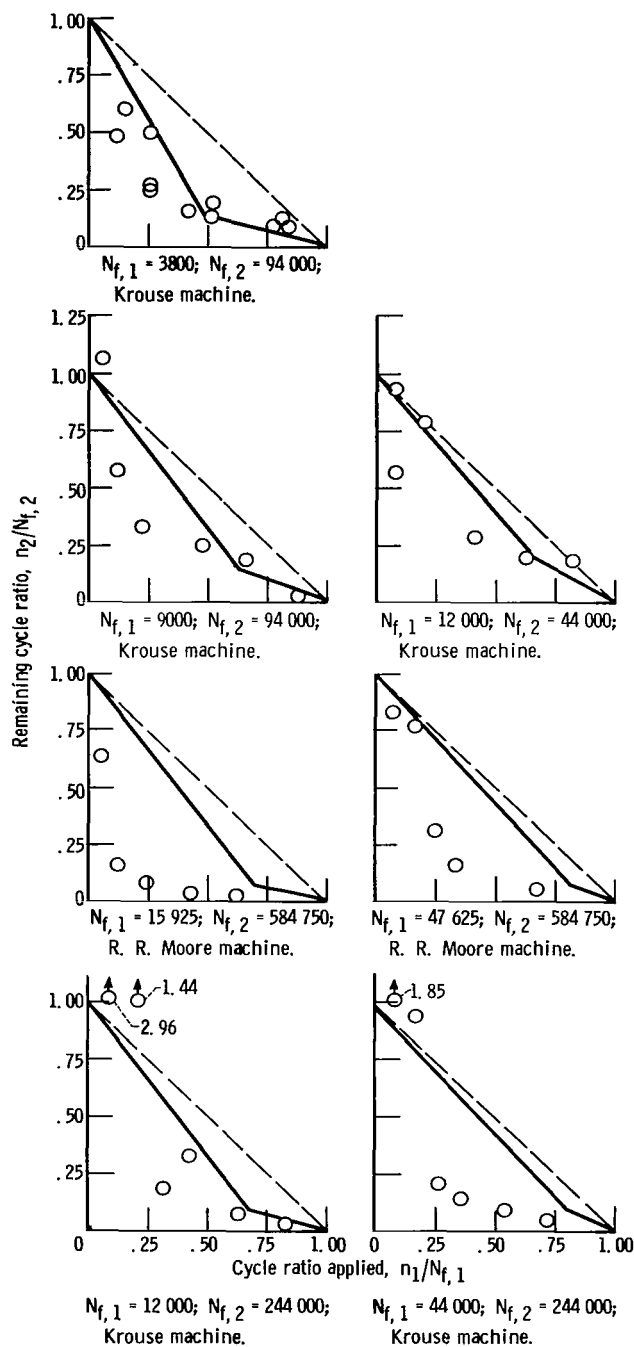
Figure 5(b) deals with the same material but considers other combinations of test conditions in which the initial life level is relatively high. The greatest discrepancies between experimental data and predicted fatigue behavior by the double linear damage rule as originally proposed occur when both the initial and the final life levels are high. The double linear damage rule would be expected to predict almost the same fatigue behavior as the conventional linear damage rule because the crack propagation period as determined from equation (1) would be relatively small. This behavior is readily seen by using equation (1) for values of $N_{f,1}$ of 15 925, 47 625, 44 000, etc. , specific conditions which are considered in figure 5(b). The experimental data show appreciably lower values of remaining cycle ratio $n_2/N_{f,2}$ than would be expected by either rule.

Figure 5(c) illustrates the results obtained under conditions of axial strain cycling with maraging steel. The initial life level was chosen in all cases to be less than 730 cycles. For this case the major part of the fatigue life would be taken up by the crack-propagation period according to the expressions thus far assumed for crack propagation and initiation in applying the double linear damage rule. Since there is essentially no crack-initiation stage, the predictions by the double linear damage rule should coincide with those by the conventional linear damage rule. These predictions did coincide for the



(a) Krouse rotating bending, high to low stress with low initial life.

Figure 5. - Comparison of predicted fatigue behavior by conventional and double linear damage rules with experimental data for two-stress (strain)-level tests. Material, maraging steel.



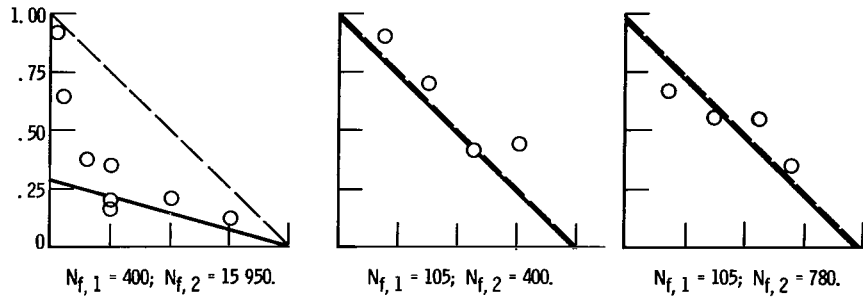
(b) Rotating bending, high to low stress with high initial life.

Figure 5. - Continued.

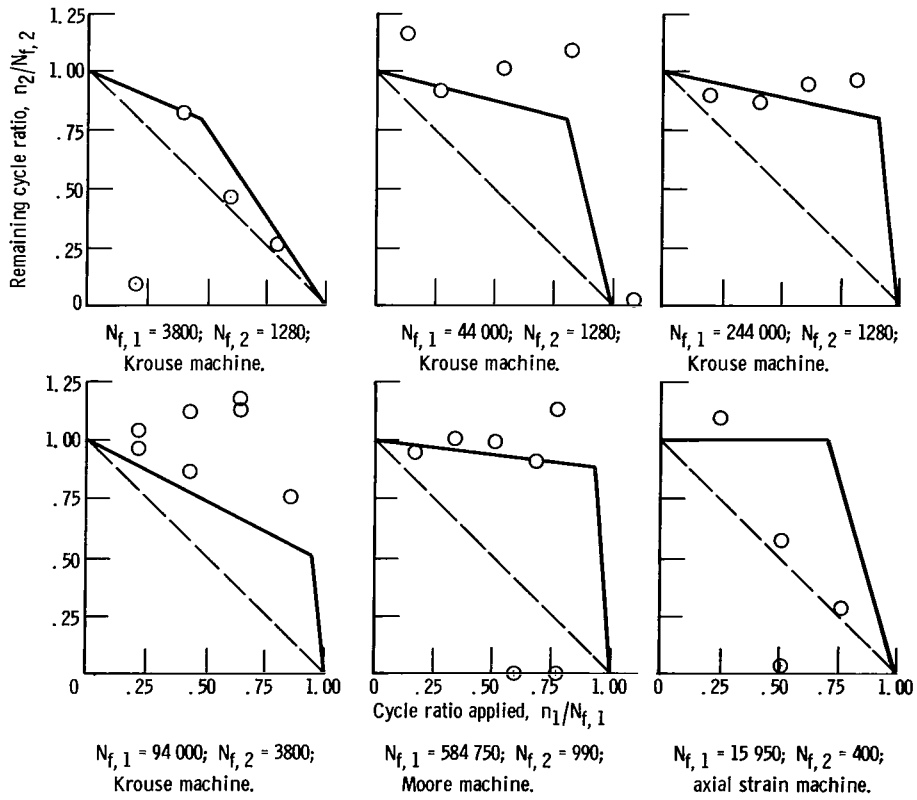
two conditions in which the final stress level was so chosen as to give a low value of life $N_{f,2}$, and the experimental data agreed well with the predictions. When the second stress level was so chosen as to give a long life, $N_{f,2} = 15\,950$ cycles, however, the predicted fatigue life by the double linear damage rule was less than that obtained experimentally. From figures 5(b) and (c), it is apparent that the experimental data fall on both sides of the predictions made by the double linear damage rule when the expression $14 N_f^{0.6}$ was used to represent the crack-propagation stage.

Thus far, consideration has been given only to the general case in which the high stress or strain (for strain cycling tests) was applied first. Figure 5(d) illustrates the opposite case in which the low stress or strain was applied first. Except for the single axial strain cycling case and one case of the rotating bending tests ($N_{f,1} = 94\,000$ and $N_{f,2} = 3800$), the predictions by the double linear damage rule show general agreement with the experimental data. Regardless of deviations of individual data points from the predictions, however, the figure shows that the order effect of loading is accounted for by the double linear damage rule.

The results for SAE 4130 steel are shown in figure 6. Figure 6(a) deals with tests in which the initial life level was low and loads at the second stress level were chosen to give various life values up to 203 000 cycles. Figure 6(b) considers an initial relatively high life



(c) Axial strain cycling, high to low strain with low initial life.



(d) Rotating bending and axial strain cycling, low to high stress (strain).

Figure 5. - Concluded.

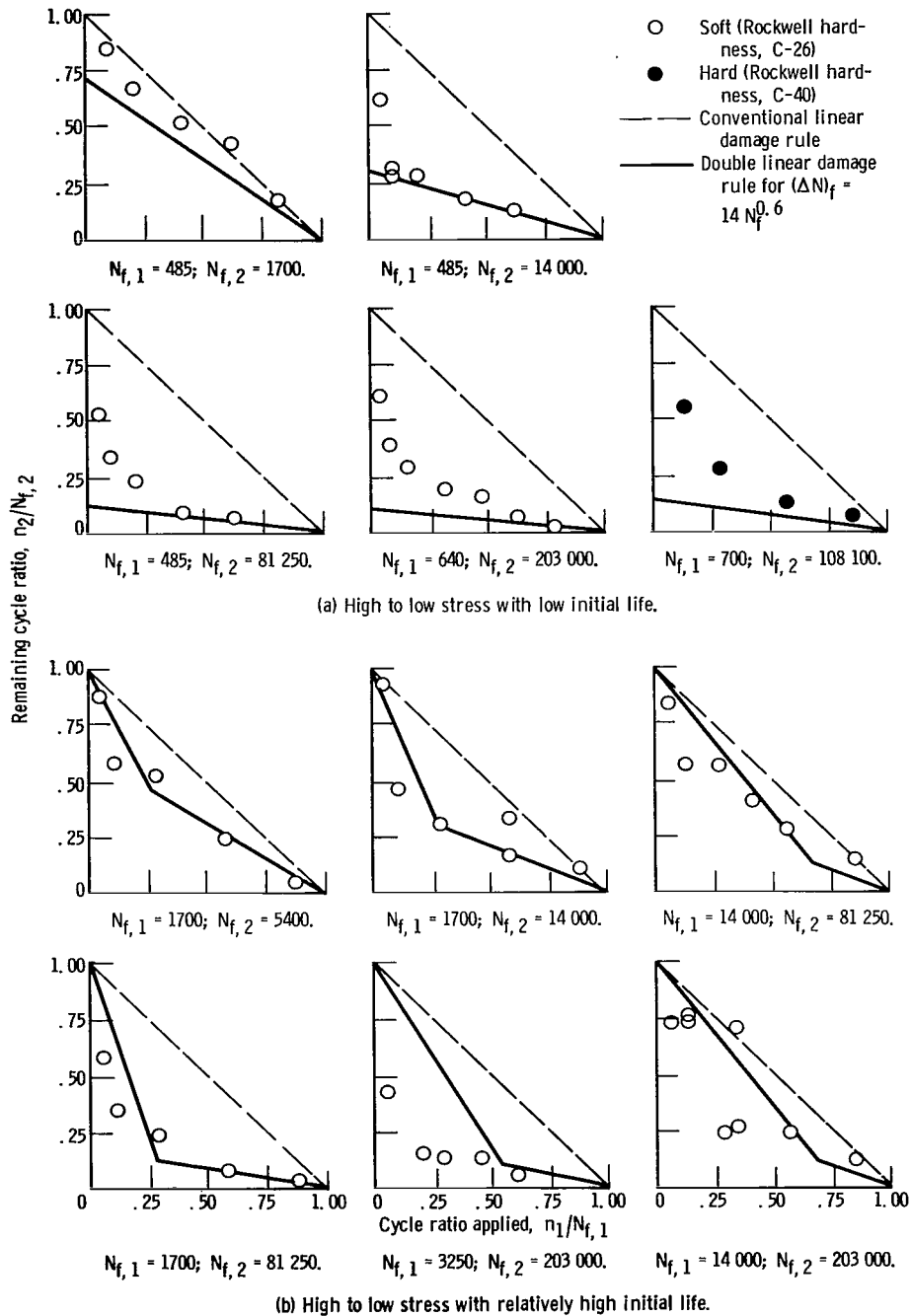


Figure 6. - Comparison of predicted fatigue behavior by conventional and double linear damage rules with experimental data for two-stress-level tests. Material, SAE 4130 steel; R. R. Moore rotating bending tests.

level. In both cases, however, the order of load application was that of high stress followed by low stress. In general, the results obtained with 4130 steel are the same as those obtained with the maraging steel for similar test conditions. For the most part, agreement between predictions by the double linear rule with $(\Delta N)_f = 14 N_f^{0.6}$ and experimental data was good, although deviations between predictions and data are clearly present in some cases. As in the case of the maraging steel, a more conservative prediction was always provided by the double linear damage rule than by the conventional linear damage rule when the high stress was applied first if the expression $14 N_f^{0.6}$ was assumed to be representative of the crack propagation stage.

Examination of the Assumed Relation for Crack Propagation $(\Delta N)_f$

In view of the deviations noted between predictions and experimental results, closer examination of the assumption that the crack-propagation period $(\Delta N)_f$ may be expressed by the relation $14 N_f^{0.6}$ was clearly in order. Before considering the possibility of improving this relation by changing the coefficient or exponent or both, however, attempts were made to determine experimentally if the propagation period $(\Delta N)_f$ was uniquely dependent upon fatigue life, N_f . The results of one such investigation are shown in figure 7. Values of ΔN_1 and ΔN_2 were obtained from two-stress-level tests with SAE 4130 soft steel in which $N_{f,1}$ was 485 cycles and $N_{f,2}$ was 14 000 cycles with the use of the graphical method previously described and illustrated in figure 1 (p. 4). These values are plotted in figure 7 as points B and A'. The values of ΔN_1 and ΔN_2

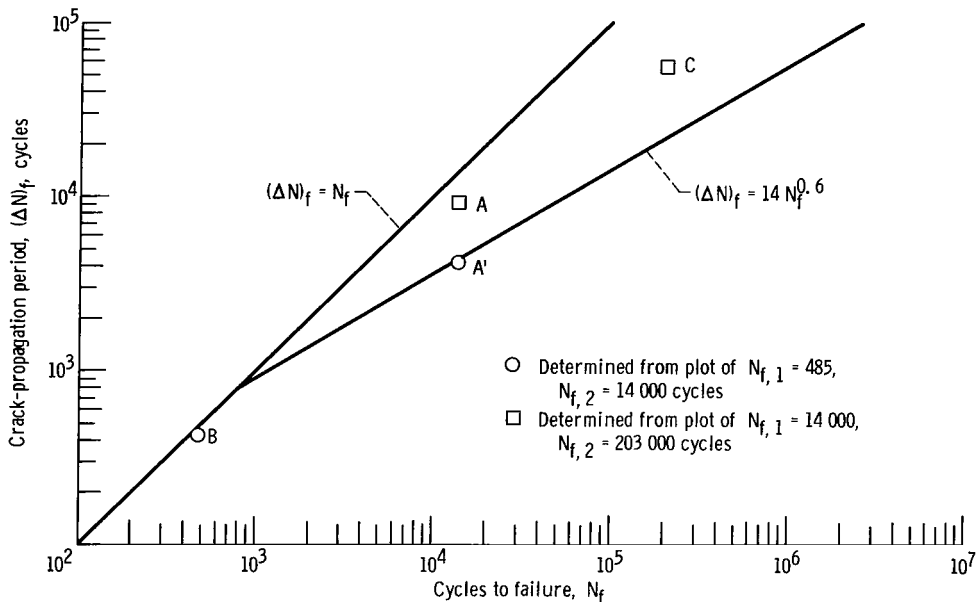


Figure 7. - Effect of stress combinations in determination of crack-propagation period. Material, 4130 soft steel; R. R. Moore rotating bending tests.

similarly obtained from another set of data in which $N_{f,1}$ was 14 000 cycles and $N_{f,2}$ was 203 000 cycles are also plotted in figure 7 as points A and C. Obviously, points A' and A, both of which relate to determinations for a life of 14 000 cycles, do not coincide as they would be expected to if ΔN were solely a function of N_f . Thus, whether a given stress (corresponding to a fixed life) is used as the first or the second stress in a two-stress-level fatigue test is clearly significant, and entirely different results can be obtained. If the representation of the crack-propagation period by the expression $14 N_f^{0.6}$ were correct, the points determined as previously mentioned would fall on the line with a slope of 0.6 when N_f values were greater than 730 cycles. It must therefore be concluded that the concept of representing crack propagation by a universal relation in terms of N_f , whether the coefficient is 14 or any other number, produces some discrepancies. Other tests of the same type for other combinations of stress were also made, which gave similar results to those shown in figure 7.

There are probably several reasons why the crack-propagation period is not uniquely

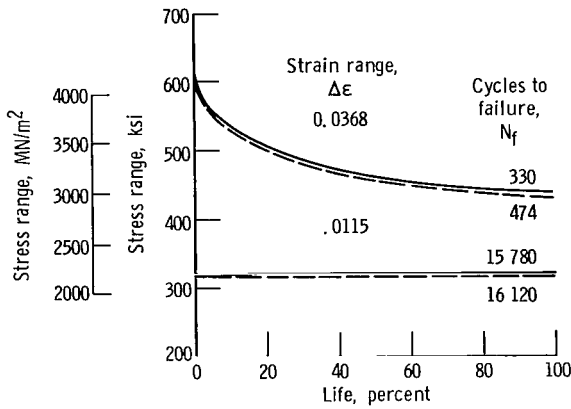


Figure 8. - Stress response in axial strain cycling for constant strain amplitude tests of maraging steel.

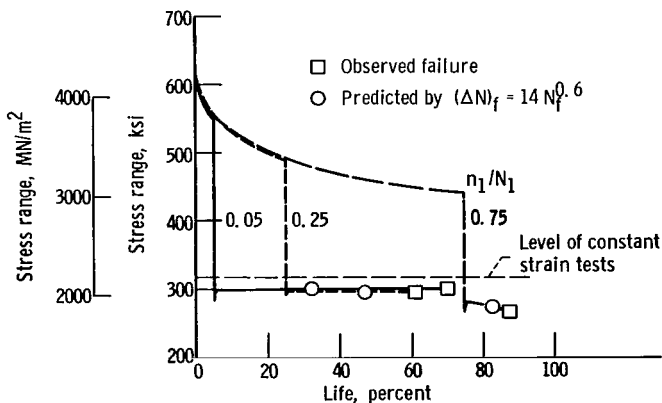


Figure 9. - Stress response in axial strain cycling two-strain-level tests of maraging steel.

related to total fatigue life (i. e., life to failure of the specimen). Reexamination is in order of the concepts that the effective crack length for crack initiation is the same at all stress levels and that extending a crack at a stress level different from that at which it was initiated is simply a continuation of the same process. The mechanisms involved are not so readily explainable. What may correspond to a crack length for effective crack initiation at one stress level may not be so at another stress level.

Another reason for the discrepancies relates to the hardening and softening characteristics of materials. Upon changing to a new strain level in a two-step test, a material that hardens or softens extensively will not reach the same stress level for a given applied strain as it would have, had that same strain been maintained throughout the test. This concept is illustrated in figures 8 and 9. Figure 8 shows the stress

response in axial strain cycling at constant strain amplitude for maraging steel. Two tests were run at each of two values of total strain. These values were chosen to give lives on the order of 400 and 16 000 cycles. Agreement between the two tests run at each condition was good and demonstrated the ability to maintain and control approximately the same strain level on the fatigue machines used. Figure 9 illustrates the stress response in axial strain cycling two-strain-level tests for maraging steel when the higher of these two-strain levels was applied first and the lower strain level subsequently applied. Maraging steel is a cyclic strain-softening material. As continually increasing percentages of the life were applied at the higher strain level, the stress required to maintain that strain level progressively decreased. Also shown on the figure are the results of running for 5, 25, and 75 percent of the total life at the initial strain followed in each case by operation to failure at the lower strain level. In each case, the stress required to maintain the lower level of constant strain in these two-step tests was lower than that required to maintain this level of strain in a single-strain-level test. Thus, the material was oversoftened as a result of the initial application of a high strain level. As a consequence, a longer life would be expected than that predicted by the double linear damage rule using the expression $14 N_f^{0.6}$ as representing the crack propagation stage. Figure 9 shows this to be true. The circles represent the predicted lives according to the double linear damage rule using $(\Delta N)_f = 14 N_f^{0.6}$; the squares represent the experimentally determined lives.

In order to describe the cumulative fatigue damage process more accurately, methods must be sought to account for the factors discussed. The double linear damage rule concept may be retained as discussed in the next section.

An Alternative Viewpoint of the Double Linear Damage Rule

In the suggested alternative approach, the concept of crack initiation and propagation in the literal sense is altered to represent two effective phases of the fatigue process, which might be designated as Phases I and II. The assumption of a linear damage rule for each of these two phases, however, would be retained. That such an assumption is reasonable may be seen by inspection of the data obtained in this investigation, particularly some of the rotating bending test results obtained with SAE 4130 steel (fig. 6(a)). These results are replotted in figure 10 to illustrate how well two straight lines originating at ordinate and abscissa values of 1.0 fit the data. The coordinates of the intersection of these lines (as defined in fig. 1) determine the values of N_0 and ΔN used to establish the fatigue curves, which represent Phases I and II of the fatigue process. In keeping with this change in concept, the form of the rule would be different for different materials and for different extreme loads that might be applied in a test. Additional

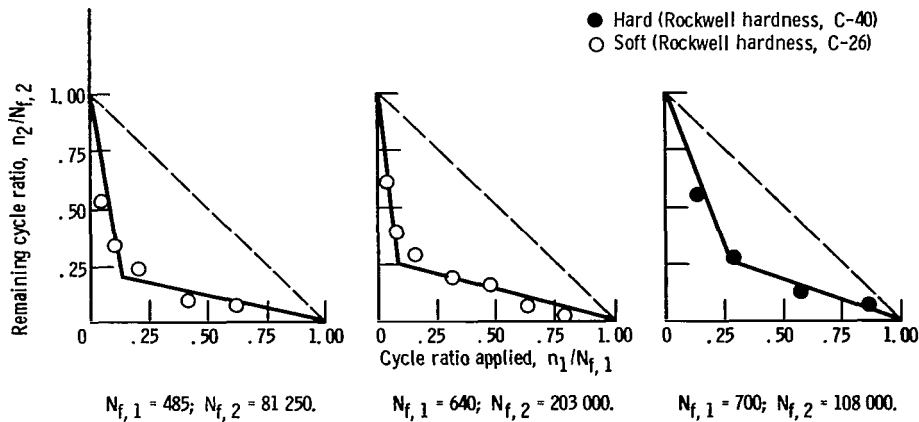


Figure 10. - Illustration of fit of two straight lines to rotating bending data obtained from two-stress-level tests with SAE 4130 steel.

experimental verification of this approach is still needed; however, the complexities discussed are accounted for in an approximate fashion. The use of a new fatigue curve different from that of the original material in predicting remaining fatigue life after prestressing is not inconsistent with other methods such as that of Corten and Dolan (ref. 4). In general, such previous approaches have assumed that the modified fatigue curves are best determined from a consideration of the highest and the lowest stress levels of the applied spectrum. This basic approach will also be adopted in the following treatment.

The double linear damage rule may be applied in the light of this revised concept to any anticipated loading spectrum for a given material if a decision is first made as to which are the highest and the lowest loads of importance. Stress levels below the fatigue limit will not be considered for the present. A series of two-stress-level tests would be run in which the highest stress level would be applied first, followed by operation to failure at the lowest stress level of significance within the loading spectrum. This procedure should bring into play the important variables such as any extremes of hardening or softening of the material and extremes of crack length involved in initiating and propagating an effective crack. From such a series of tests and for that particular combination of stress levels, the values of N_0 and ΔN may be determined for both stresses by using the graphical procedure for applying the double linear damage rule as previously described. These values may then be plotted as shown in figure 11 at the two stress levels, and curves may be sketched between these points that are consistent with the appearance of the original fatigue curve. It would then be possible to analyze by the double linear damage rule the effect of block or spectrum loading of any pattern that could also include loadings between the highest and the lowest levels. The N_0 and the ΔN curves would be used for determining the effective values of Phases I and II of the fatigue process. These curves would replace the expression $(\Delta N)_f = 14 N_f^{0.6}$ or any other variation of such a formula. One example of applying this procedure is given in appendix B.

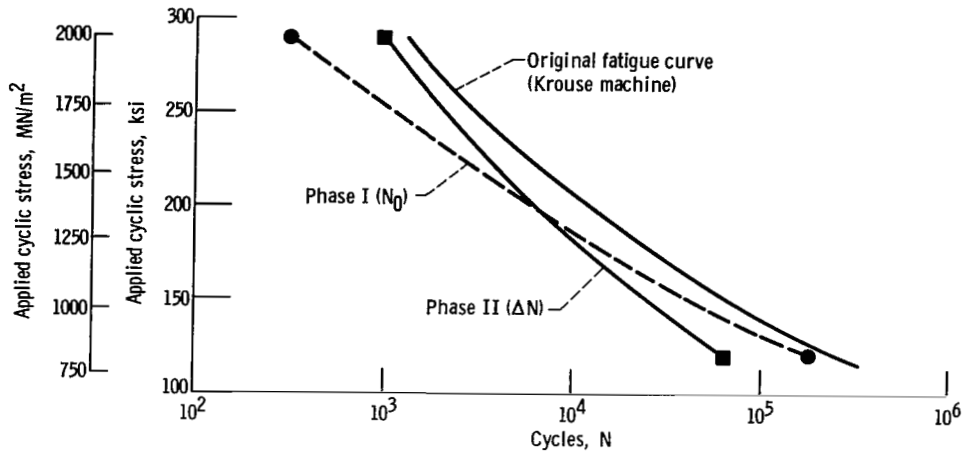


Figure 11. - Determination of Phases I and II of fatigue process from two-stress-level tests at highest and lowest stress levels of loading spectrum. Material, maraging steel.

Although at this early stage of the development of this approach, it seems most convenient to use a two-level test as illustrated in figure 1 (p. 4) to determine the effective values of Phases I and II for given extremes of stress or strain level within a given loading spectrum, further consideration may reveal better approaches for particular circumstances. For example, it may be desirable to use a block loading with the highest and the lowest significant stresses in the spectrum of service loading for establishing the point of effective transition between the two phases (point B in fig. 1), rather than merely following the high stress cycles by continuous loading at the lower stress. Since only two unknowns are involved (the points of effective transition from Phase I to Phase II for each of the two stress levels when applied in conjunction with the other), only two tests would be required to determine the two unknowns. This approach is further discussed in the CONCLUDING REMARKS.

Limited Experimental Verification of Alternative Viewpoint of Double Linear Damage Rule

In order to provide an indication of the validity of the alternative viewpoint of the double linear damage rule, a series of repetitive alternating two-stress-level block tests was conducted. Such a test may be considered as the next step in complexity to the single block two-stress-level test, which provided most of the data obtained in this investigation. The manner of conducting the test is fully described in appendix C. Briefly, a two-stress-level single block base was selected. Equal fractional portions of the number of cycles at each stress level in the block were applied in a repetitive fashion. The double linear damage rule was applied to predict the summation of the cycle ratios required to cause failure

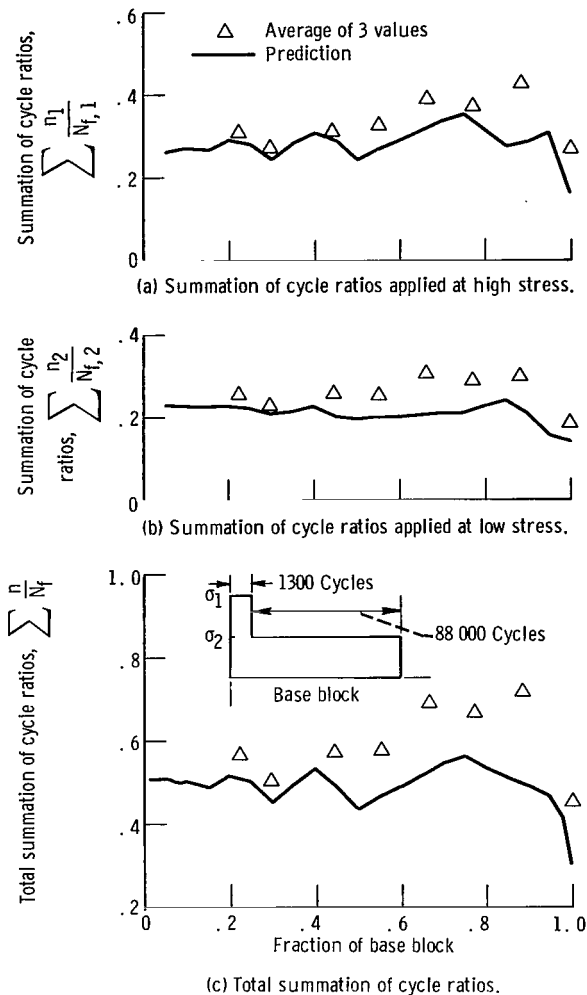


Figure 12. - Comparison of experimental and predicted summation of cycle ratios for alternating two-stress-level tests. Predictions made by double linear damage rule using experimental data to define Phases I and II of the fatigue process.

with the use of experimentally determined curves representing Phases I and II of the fatigue process. A numerical example illustrating this method is also given in appendix C.

The experimental results of these tests as well as the predictions are shown in figure 12. The summations of the cycle ratios are plotted against the fractions of the basic block considered. Figure 12(a) deals with the summation of cycle ratios applied at the high stress; figure 12(b) deals with the summation of cycle ratios at the low stress; and figure 12(c) deals with the total summation. The experimental data shown represent the arithmetic averages of three data points obtained at each fraction of the block considered. In general, reasonable agreement exists between the predicted results and the experimental data. The irregularity in the predicted results is associated with abrupt numerical changes that are introduced when predicted failure changes from the high to the low portions of the block loading pattern. In all cases, the predictions by the double linear damage rule are conservative. Much additional experimental verification is needed to establish fully the usefulness of the double linear damage rule in predicting remaining fatigue life for more complex loading spectra.

The single series of tests contained in figure 12 serves more to illustrate the approach than to prove validity of the method.

CONCLUDING REMARKS

Cumulative fatigue damage in two-stress-level tests was predicted with reasonable accuracy for smooth 1/4-inch-diameter specimens by a previously proposed method based on the concept of a double linear damage rule. While a double linear damage rule

used with the assumption that $(\Delta N)_f = 14 N_f^{0.6}$ gives better results than the conventional linear damage rule, it is not adequate where crack initiation and propagation are expressed solely in terms of total life. Other representations of crack initiation and propagation might be more accurate, but they must take into account the hardening and the softening characteristics of the material and more particularly the effect of the stress levels involved. An alternative viewpoint of the double linear damage rule, in which the concept of crack initiation and propagation in the literal sense is altered to represent two effective phases of the fatigue process designated as Phases I and II which can be determined experimentally, appears to overcome some of the limitations of the original proposal. The form of the rule then becomes different for different materials and for different extreme loads that might be applied. In principle, only two tests are required to determine the point of transition between the two effective phases of the fatigue process. The actual number of tests employed can, of course, be greater, depending on the degree of accuracy desired. A suggested approach is to conduct the first test by applying a cycle ratio $n_1/N_{f,1}$ of approximately 0.2 at the high stress and then to operate to failure at the low stress. For the second test, apply a cycle ratio $n_1/N_{f,1}$ of approximately 0.5 at the high stress before running to failure at the low stress. Two straight lines emanating from ordinate and abscissa values of one on a plot of $n_2/N_{f,2}$ against $n_1/N_{f,1}$ may then be drawn, each of which passes through one of the data points describing these tests. The coordinates of the intersection of these two straight lines will determine the values of N_0 and ΔN used to establish the fatigue curves which represent Phases I and II of the fatigue process.

It is emphasized that the purpose of the two-step test is to provide a determination of the transition between these two phases of fatigue and, thereby, to enable the investigator to construct effective fatigue curves for each phase as shown in figure 11. Once these two curves are constructed, their application is intended for all spectrums of loading involving as loading extremes the two stresses used for their determination. Thus, use of these curves is not limited to two-step tests. Until further research is conducted to extend the application, the procedure must be limited to the study of smooth 1/4-inch-diameter specimens. It may, however, be regarded as a first step in the direction of eventually predicting the effect of a complex loading history on the life of more complex structures.

Lewis Research Center,
National Aeronautics and Space Administration,
Cleveland, Ohio, October 14, 1966,
129-03-15-06-22.

APPENDIX A

APPLICATION OF DOUBLE LINEAR DAMAGE RULE TO A TWO-STRESS- LEVEL TEST USING THE RELATION $14 N_f^{0.6}$ TO DEFINE THE CRACK PROPAGATION PERIOD

Two stress levels 1 and 2, at which the total lives of the original material are $N_{f,1}$ and $N_{f,2}$, respectively, and a prestress cycle ratio $n_1/N_{f,1}$ are given; it is desired to find the number of cycles that can be applied at the second stress level. The values of ΔN_1 and ΔN_2 are first determined from equation (1). The values of $N_{o,1}$ and $N_{o,2}$ can then be obtained with the use of equation (2). Next, the ratio $N_{o,1}/N_{f,1}$ is determined. Where $N_{f,1} > 730$ cycles, if $n_1/N_{f,1}$ is equal to $N_{o,1}/N_{f,1}$, the crack-initiation stage has just been completed, and the cyclic life remaining at the second stress level is exactly equal to that making up the crack-propagation period, or

$$n_2 = N_{f,2} - N_{o,2} = \Delta N_2 \quad (A1)$$

If the ratio $n_1/N_{f,1} > N_{o,1}/N_{f,1}$, the life remaining at the second stress level may be expressed as

$$n_2 = \left(1 - \frac{n_1 - N_{o,1}}{\Delta N_1}\right) \Delta N_2 \quad (A2)$$

If the ratio $n_1/N_{f,1} < N_{o,1}/N_{f,1}$, the life remaining at the second stress level may be expressed as

$$n_2 = \left(1 - \frac{n_1}{N_{o,1}}\right) N_{o,2} + \Delta N_2 \quad (A3)$$

Where $N_{f,1} < 730$ cycles, it is assumed that there is no lengthy crack-initiation period, but rather that total life consists only of crack propagation. Then, the life remaining at the second stress level can be determined from the expression

$$n_2 = \left(1 - \frac{n_1}{N_{f,1}}\right) \Delta N_2 \quad (A4)$$

In effect then for the latter case, total life at stress 2 is determined from the linear damage rule for crack propagation only.

APPENDIX B

APPLICATION OF DOUBLE LINEAR DAMAGE RULE USING EXPERIMENTAL DATA TO DEFINE PHASES I AND II OF FATIGUE PROCESS

In this appendix, detailed examples are given to show how the Phase I and Phase II curves of figure 11 (p. 18) were obtained and how these curves might possibly be used to predict the life of a three-stress-level fatigue test.

To define the two phases of the fatigue process, some two-stress-level tests must first be conducted with the use of the highest and the lowest stresses of importance in the particular loading spectrum under consideration. For this illustration, the material chosen was the maraging steel, and the two stresses chosen were 290 000 psi (2000 MN/m²) and 120 000 psi (827 MN/m²). From the original fatigue curve of figure 11 for this material (obtained on a Krouse machine), $N_{f,1}$ and $N_{f,2}$ equal 1280 and 244 000 cycles, respectively. The data obtained from a series of tests conducted by applying various cycle ratios $n_1/N_{f,1}$ at the high stress and operating to failure at the low stress are plotted in figure 13. Straight lines were then fitted through the data. These lines were required to originate from cycle-ratio values of 1.0 on the ordinate and the abscissa. The coordinates of the intersection point B are $n_1/N_{f,1}$ and $n_2/N_{f,2}$ and have numerical values of 0.25 and 0.24, respectively. Since these ratios are equivalent to $N_{o,1}/N_{f,1}$ and $\Delta N_2/N_{f,2}$ as shown in figure 1 (p. 4), the values of $N_{o,1}$, ΔN_1 , $N_{o,2}$, and ΔN_2 were calculated to be 320, 960, 185 000, and 59 000 cycles, respectively. These values

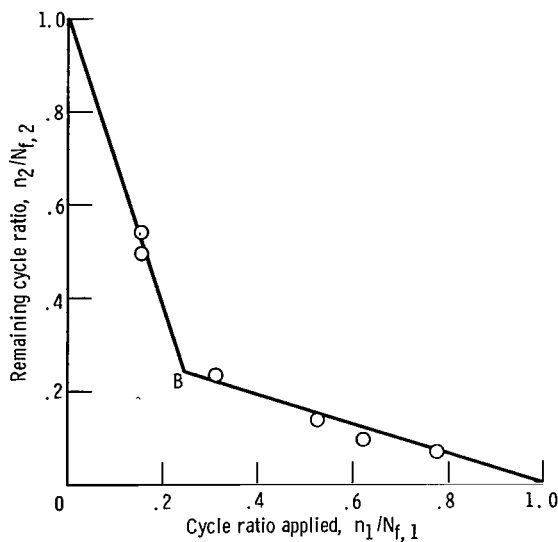


Figure 13. - Two straight lines fitted to data from two-stress-level tests of maraging steel. $N_{f,1} = 1280$; $N_{f,2} = 244\ 000$.

were then plotted at their corresponding stresses as shown in figure 11 and were connected by curves, the shapes of which are guided by the shape of the original fatigue curve. These curves may then be used in separate linear summations for Phases I and II of the fatigue process.

As a numerical example of the method of applying the double linear damage rule using these Phase I and Phase II curves, a three-stress-level test in which the highest and the lowest stresses are 290 000 and 120 000 psi is considered. It is required to predict the remaining life at a third stress level, 200 000 psi (1380 MN/m²), after 200 and 40 000 cycles, respectively, have been applied at the

highest and the lowest stresses. Values of $N_{O,3}$ and ΔN_3 can be obtained from the Phase I and Phase II curves of figure 11. Thus, $N_{O,3}$ equals 5900 cycles and ΔN_3 equals 6100 cycles. The application of 200 cycles at stress 1 results in a ratio of

$$\frac{n_1}{N_{O,1}} = 0.63 < 1$$

which indicates that Phase I has not been completed and that it is continued at the second stress level. The application of 40 000 cycles at the second stress results in a ratio of

$$\frac{n_2}{N_{O,2}} = 0.22$$

Summing the cycle ratios applied at stresses 1 and 2 results in

$$\frac{n_1}{N_{O,1}} + \frac{n_2}{N_{O,2}} = 0.63 + 0.22 = 0.85 < 1$$

The portion x of the number of cycles applied at stress 3 needed to complete Phase I is, from equation (3),

$$\frac{x}{N_{O,3}} = 1 - \left(\frac{n_1}{N_{O,1}} + \frac{n_2}{N_{O,2}} \right)$$

or

$$x = 885 \text{ cycles}$$

The portion of the number of cycles applied at stress 3, that is needed to complete Phase II is, from equation (4),

$$\frac{y}{6100} = 1$$

or

$$y = 6100 \text{ cycles}$$

Then, the total number of cycles remaining at the third stress level is equal to

$$x + y = 885 + 6100 = 6985 \text{ cycles}$$

APPENDIX C

APPLICATION OF DOUBLE LINEAR DAMAGE RULE TO ALTERNATING TWO-STRESS-LEVEL TESTS IN WHICH EXPERIMENTAL DATA ARE USED TO DEFINE PHASES I AND II OF FATIGUE PROCESS

Alternating two-stress-level tests were conducted as follows: Initially, two-stress-level tests were conducted at various cycle ratios, $n_1/N_{f,1}$, at a high stress, 190 000 psi (1310 MN/m²), and the remaining cyclic life ratios $n_2/N_{f,2}$ were determined at a second stress, 110 000 psi (785 MN/m²). At 190 000 psi, $N_{f,1}$ was 8000 cycles. At 110 000 psi, $N_{f,2}$ was 625 000 cycles. These N_f values were obtained with specimens from a different heat of maraging steel from that for which the R. R. Moore machine data previously described herein for this material were obtained. The results of the tests in which different cycle ratios were applied at 190 000 psi were plotted as shown in figure 14. Best visual-fit straight lines were drawn through the data, which again met the requirement that they originate from a value of cycle ratio of 1.0 on the ordinate and the abscissa. From the coordinates of the intersection point B and the values of $N_{f,1}$ and $N_{f,2}$, the Phase I and Phase II parameters were determined. Thus, $N_{o,1}$ equaled 1300 cycles; ΔN_1 , 6700 cycles; $N_{o,2}$, 537 000 cycles; and ΔN_2 , 88 000 cycles. Several alternating two-stress-level block tests were then specified such that various fractions of 1300 cycles were applied at the high stress of 190 000 psi and identical fractions of 88 000 cycles were applied at the low stress.

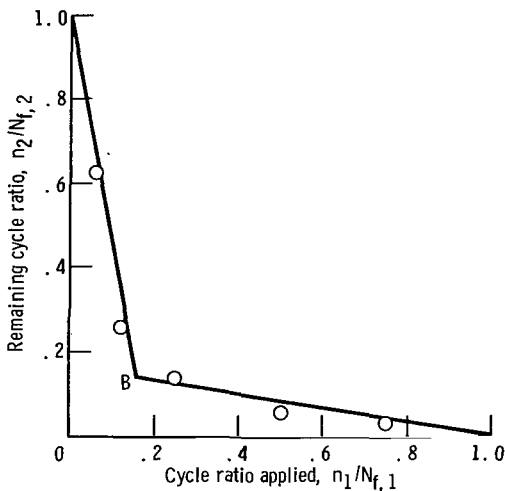


Figure 14. - Experimental determination of Phase I and Phase II transition used in conjunction with double linear damage rule. Material, maraging steel; $N_{f,1} = 8000$; $N_{f,2} = 625\ 000$.

The following numerical example illustrates the manner of applying the double linear damage rule to an alternating two-stress-level test. The example considers an alternating block test in which the alternating or repeated block is taken to be one-half of the number of cycles at each stress level in the base block. Both the base block and the alternating half block are shown diagrammatically in figure 15. The base block for this example (as well as for all tests of fig. 12, p. 19) is defined as consisting of 1300 cycles at the first stress and 88 000 cycles at the second stress. To determine the number of cycles to complete Phase I equation (3) is applied. Since

$$\frac{650}{1300} + \frac{44\ 000}{537\ 000} < 1$$

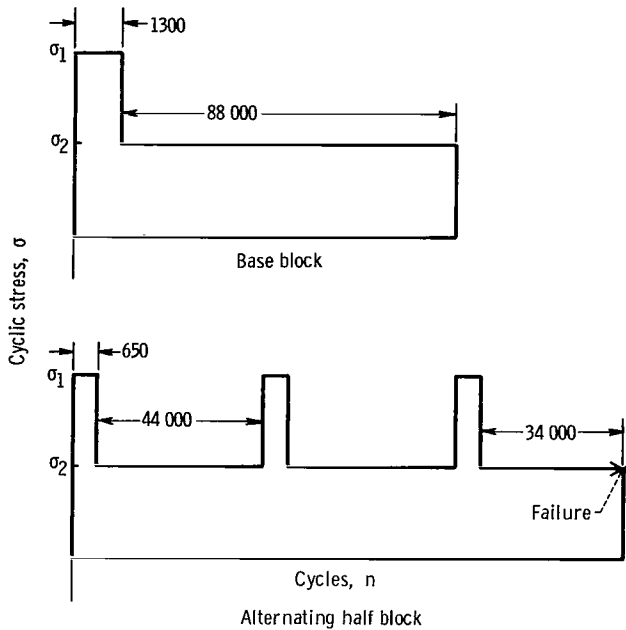


Figure 15. - Diagram of loading pattern for numerical example of appendix C.

it is apparent that Phase I has not been completed in the first loading block. To determine if Phase I is completed in the high-stress portion of the second loading block, again equation (3) is applied:

$$\frac{650}{1300} + \frac{44\,000}{537\,000} + \frac{x}{1300} = 1$$

or $x = 543$ cycles, at which Phase I is complete. Next, the number of cycles needed to complete Phase II is determined. Equation (4) is applied to determine whether Phase II is completed in the second loading block. This application gives

$$\frac{650 - 543}{6700} + \frac{44\,000}{88\,000} < 1$$

which indicates that Phase II has not been completed in block 2. Therefore, it is necessary to determine whether Phase II is completed in the high-stress portion of block 3. Thus,

$$\frac{650 - 543}{6700} + \frac{44\,000}{88\,000} + \frac{y}{6700} = 1$$

and

$$y = 3243$$

Since $y > 650$, Phase II has not been completed in the high-stress portion of block 3, and the next step is to determine whether it is completed in the low-stress portion of this block. Thus,

$$\frac{650 - 543}{6700} + \frac{44\,000}{88\,000} + \frac{650}{6700} + \frac{z}{88\,000} = 1$$

and $z = 34\,000$. Since $z < 44\,000$ cycles, Phase II has been completed, and failure occurs during the low-stress portion of block 3. The total summation of cycle ratios $\sum n/N_f$ for this example then is

$$\sum \frac{n}{N_f} = \frac{650}{8000} + \frac{44\,000}{625\,000} + \frac{650}{8000} + \frac{44\,000}{625\,000} + \frac{650}{8000} + \frac{34\,000}{625\,000} = 0.44$$

In the same manner, other apportionments of the cycles sustained at the intersection point of a two-stress-level test (analogous to point B of fig. 1, p. 4) can be computed, and the expected number of cycles to failure can be predicted for alternating block loading applications.

REFERENCES

1. Kaechele, Lloyd: Review and Analysis of Cumulative-Fatigue-Damage Theories. Rep. No. RM-3650-PR, Rand Corp., Aug. 1963.
2. Richart, F. E., Jr.; and Newmark, N. M.: An Hypothesis for the Determination of Cumulative Damage in Fatigue. ASTM Proc., vol. 48, 1948, pp. 767-800.
3. Marco, S. M.; and Starkey, W. L.: A Concept of Fatigue Damage. ASME Trans., vol. 76, no. 4, May 1954, pp. 627-632.
4. Corten, H. T.; and Dolan, T. J.: Cumulative Fatigue Damage. International Conference on Fatigue of Metals. Vol. 1. Inst. of Mech. Engrs., 1956, Session 3, paper no. 2.
5. Freudenthal, Alfred M.; and Heller, Robert A.: On Stress Interaction in Fatigue and a Cumulative Damage Rule. Part I - 2024 Aluminum and SAE 4340 Steel Alloys. (WADC TR 58-69, pt. 1, DDC No. AD-155687), Columbia Univ., June 1958.
6. Palmgren, Arvid: Die Lebensdauer von Kugellagern. Z. Ver. Deut. Ing., vol. 68, no. 14, Apr. 5, 1924, pp. 339-341.
7. Miner, Milton A.: Cumulative Damage in Fatigue. J. Appl. Mech., vol. 12, no. 3, Sept. 1945, pp. 159-164.
8. Henry, D. L.: A Theory of Fatigue-Damage Accumulation in Steel. ASME Trans., vol. 77, no. 6, Aug. 1955, pp. 913-918.
9. Manson, S. S.; Nachtigall, A. J.; and Freche, J. C.: A Proposed New Relation for Cumulative Fatigue Damage in Bending. ASTM Proc., vol. 61, 1961, pp. 679-703.
10. Manson, S. S.; Nachtigall, A. J.; Ensign, C. R.; and Freche, J. C.: Further Investigation of a Relation for Cumulative Fatigue Damage in Bending. J. Eng. Industry, vol. 87, no. 1, Feb. 1965, pp. 25-35.
11. Rally, F. C.; and Sinclair, G. M.: Influence of Strain Aging on the Shape of the S-N Diagram. Rep. No. 87, Dept. of Theoretical and Appl. Mechanics, Univ. of Illinois, June 1955.
12. Grover, Horace J.: An Observation Concerning the Cycle Ratio in Cumulative Damage. Symposium on Fatigue of Aircraft Structures. Spec. Tech. Publ. No. 274, ASTM, 1960, pp. 120-124.
13. Manson, S. S.: Interfaces between Fatigue, Creep, and Fracture. Intern. J. Fracture Mech., vol. 2, no. 1, Mar. 1966, pp. 327-363.

14. Manson, S. S.; and Hirschberg, M. H.: Prediction of Fatigue of Notched Specimens by Consideration of Crack Initiation and Propagation. NASA TN D-3146, 1966.
15. Smith, Robert W.; Hirschberg, Marvin H.; and Manson, S. S.: Fatigue Behavior of Materials Under Strain Cycling in Low and Intermediate Life Range. NASA TN D-1574, 1963.

TABLE I. - MATERIAL DESCRIPTION

Material	Nominal composition, weight percent	Condition	Hardness, Rockwell C -
4130 (soft)	C, 0.030; Mn, 0.50; P, 0.040; S, 0.040; Si, 0.28; Cr, 0.95; Mo, 0.20; Fe remainder	1700° F, 1/2 hr in salt, water quench; 1200° F, 1/2 hr in salt, air cool	25 to 27
4130 (hard)	C, 0.030; Mn, 0.50; P, 0.040; S, 0.040; Si, 0.28; Cr, 0.95; Mo, 0.20; Fe remainder	1600° F, 1/2 hr in salt, water quench; 750° F, 1 hr in salt, air cool	39 to 40
Maraging steel	C, 0.03 max.; Si, 0.10 max.; Mn, 0.10 max.; S, 0.010 max.; P, 0.010 max.; Ni, 18.50; Co, 9.00; Mo, 4.80; Al, 0.10; Ti, 0.60; B, 0.003; Zr, 0.02 added; Ca, 0.05 added	1500° F, 3/4 hr, air cool; 900° F, 3½ hr, air cool	52
		1700° F, 1/2 hr, air cool; 1500° F, 1 hr, air cool; 900° F, 3½ hr, air cool	

^aHeat treatment for material used in R. R. Moore and axial tests.

^bHeat treatment for material used in Krouse tests and R. R. Moore tests of specimens designated R, S, T, U, or V in tables III, V, and VII.

TABLE II. - TENSILE PROPERTIES OF TEST MATERIALS

Material	Yield strength, 0.2 percent offset, ksi (a)	Ultimate strength, ksi (a)	Fracture strength, ksi (a)	Reduction in area, percent	Modulus of elasticity, ksi (a)
4130 (soft)	113	130	245	67.3	32×10 ⁶
4130 (hard)	197	207	302	54.7	29
Maraging steel	---	295	380	50.7	27

^aMultiply by 6.8948 to convert to MN/m².

TABLE III. - ROTATING BENDING FATIGUE TEST DATA OBTAINED AT CONSTANT NOMINAL STRESS AMPLITUDE

Specimen	Stress level, ksi (a)	Test frequency, rpm (b)	Cycles to failure	Specimen	Stress level, ksi (a)	Test frequency, rpm (b)	Cycles to failure	Specimen	Stress level, ksi (a), (d)	Test frequency, rpm (b)	Cycles to failure
Maraging steel; Krouse machine				Maraging steel; Krouse machine				Maraging steel; R. R. Moore machine			
8R16	290	100	1117	8G16	200	5000	13100	8A37	300AC	1000	625
8K7	240	100	1166	8K17	200	5000	13700	8A37	300AC	1000	700
8C5	290	100	1203	8H2	200	5000	13800	8C32	300	100	836
8P14	290	100	1267	8G10	200	3000	14100	8C18	300	100	915
8H6	240	100	1307	dJ15	200	5000	15000	8C22	300AC	100	942
8J12	290	100	1356	8F3	180	3000	19300	8C2	300AC	100	991
8N17	290	100	1369	8H13	180	5000	20400	8A38	300AC	100	1060
8L14	290	100	1392	8015	180	3000	23200	8A11	290AC	100	1201
8K16	290	1000	1400	8F11	170	5000	32700	8C12	240	1000	825
8F13	270	100	1741	8C1	170	5000	38900	894	280AC	1000	1725
8G3	270	100	1807	8E7	170	5000	42300	891	290AC	1000	1825
8G1	270	100	1918	8A11	160	5000	42500	8A22	260	100	2043
8J3	270	100	1994	8D11	160	5000	47500	87	260	100	2160
8F3	270	100	2129	8G18	160	3000	50000	8321	260	100	2502
807	270	100	2187	8K3	160	5000	63000	8A14	260AC	1000	2830
8013	266	100	2100	8F5	160	5000	75500	8A39	260AC	1000	3150
8L18	266	100	2357	8F7	160	5000	82600	8C4	240AC	1000	5050
8M7	266	100	2415	8F1	160	3000	224100	8A20	240AC	1000	5425
8C3	260	5000	2000	8C9	150	4000	70900	8A3	220	100	5527
8H17	260	100	2166	8E14	140	5000	54600	8A11	220	100	5994
8A10	260	5000	2200	8H7	140	5000	94100	8C26	220AC	1000	7575
8G2	250	100	2230	8J14	140	5000	92100	8C31	220AC	1000	7975
8G7	260	100	2394	8K5	140	5000	103000	8A19	200	1000	9000
8E10	260	100	2561	8G12	140	5000	149500	8B29	200	1000	9500
8E1	260	100	2663	8H12	120	5000	76800	8A17	200	1500	10770
801	260	100	2695	8H14	120	5000	100400	899	200AC	1000	13125
896	250	100	2917	8A9	120	5000	140200	8A13	200AC	1000	13200
8J4	250	5000	3000	8C6	120	5000	232800	8A19	190	1500	11800
8C2	250	100	3018	8K11	120	5000	346400	8C33	190AC	1000	13275
8F13	250	100	3062	8A2	120	5000	380800	8A30	190AC	1000	15925
8H4	240	100	3000	8D8	120	5000	836000	8A25	190AC	1000	16425
8A15	240	100	3315	8M14	110	5000	472600	8A10	180	2000	15500
8A16	240	100	3417	8L10	110	5000	475000	8A39	180	2000	17000
8B1	240	100	3559	804	110	5000	814500	8C21	180	2000	18600
8G4	240	100	3713	8M15	105	5000	660300	8C24	180	1600	18650
8K4	240	1000	3800	8D7	105	5000	766600	8C34	180AC	1000	25200
8Y3	240	5000	4000	8B14	105	5000	1555400	8B28	180AC	1000	26775
8A4	240	5000	4100					8A16	170	2000	29500
8F10	240	3000	4200					8B20	160	2000	32250
8F14	240	5000	4800					8C25	160	1800	33250
8J2	240	3000	4800					8C16	160	2000	34250
8K13	220	5000	5600					8C10	160	2000	42680
8J8	220	3000	7200					8A33	160AC	1000	44000
8C4	210	3000	7500					8A40	160AC	1000	47625
8C10	210	3000	8300					8C6	160AC	1000	79825
8F9	210	3000	11000					8A28	140	2000	44000
801	200	3000	11500					8A8	140	1800	165500
8P16	200	3000	12100					8B26	140AC	3000	292700
8G11	200	4000	12200					8C11	130AC	5000	251000

^aMultiply by 6.8948 to convert to MN/m².

^bMultiply by 0.0167 to convert to Hz.

^cSpecimens with letter designations R, S, T, U, or V were from a different heat, and these data were used only in appendix C.

^dThe letters AC designate air-cooled specimen.

TABLE III. - Continued. ROTATING BENDING FATIGUE TEST DATA OBTAINED AT CONSTANT NOMINAL STRESS AMPLITUDE

Specimen (c)	Stress level, ksi (a), (d)	Test frequency, rpm (b)	Cycles to failure	Specimen	Stress level, ksi (a), (d)	Test frequency, rpm (b)	Cycles to failure	Specimen	Stress level, ksi (a), (d)	Test frequency, rpm (b)	Cycles to failure
Maraging steel; R. R. Moore machine				SAE 4130 (soft) steel; R. R. Moore machine				SAE 4130 (soft) steel; R. R. Moore machine			
8R36	130AC	2000	406700	2M6	160	500	225	P26	110	5000	8000
8R27	130AC	5000	534750	2M33	160	500	250	Q29	110	200	8549
8A36	130AC	5000	855000	2M28	160	500	250	Q33	110	5000	10000
8A31	130AC	5000	1570250	2K25	150AC	100	391	Q10	110	5000	11750
8A10	124AC	5000	9631250	1S3	140AC	100	412	Q22	100	100	11158
8A17	120AC	5000	2296000	A11	140	500	450	1S18	100AC	3000	11250
8B5	120AC	5000	4399500	1S30	140AC	100	485	1T12	100AC	3000	14000
4C15	116AC	5000	989000	1T33	140AC	100	540	V32	100	5000	15000
8A9	116AC	5000	2772000	M22	140	500	550	1S11	100AC	2000	15525
8338	112AC	5000	80750	2J25	140AC	100	610	2M20	100	5000	16000
8A15	112AC	5000	2537000	2D10	140AC	100	669	2M1	100	5000	17500
8A19	112AC	5000	7093500	2N8	140AC	100	711	S6	100	5000	19000
8332	112	5000	9999999	2M16	140AC	500	725	S38	100	5000	19000
8C5	112	5000	9999999	2A3	140AC	500	750	S37	100	5000	19000
8U12	140AC	100	6237	2M29	140AC	500	775	2L39	100	5000	19700
4V8	140AC	100	7792	2M31	140AC	500	825	P2	100	10000	19750
8P14	140AC	100	7999	2A31	140AC	500	850	T37	100	5000	20000
8U11	140AC	100	8720	1S21	120AC	100	1670	Q24	100	5000	21000
4T11	140AC	100	9570	1S32	120AC	100	1678	2M12	100	5000	21250
8R15	140AC	1000	11275	1S4	120AC	1000	1700	2D8	100	5000	22000
8U16	140AC	1000	12675	1T13	120AC	100	1842	2K5	100	5000	22250
8U10	140AC	1000	13150	1T16	120AC	100	1992	Q5	100	5000	23000
8R2	130AC	7000	49000	Q7	120	5000	2000	T5	100	5000	24000
4T10	130AC	5000	53750	2M30	120AC	5000	2250	Z30	100	5000	25000
8V16	130AC	5000	59000	2M23	120AC	100	2317	2K4	100AC	5000	27500
8R16	130AC	8000	60250	Q22	120	5000	2500	2M11	100AC	5000	29250
4S10	130AC	5000	66750	2M4	120AC	5000	2500	2M27	100AC	5000	31750
8V7	130AC	5000	75000	2N3	120AC	5000	2500	P3	100	5000	33500
8S5	130AC	5000	88000	2D26	120AC	100	2506	Q35	100	5000	34000
4S10	130AC	7000	178500	2L13	120AC	5000	2750	2L7	100AC	5000	41500
4V4	130AC	5000	225500	2034	120AC	1000	2950	P30	100	5000	45700
8U8	130AC	5000	321250	2M32	120AC	500	3025	Q37	95	5000	37000
4S13	120AC	5000	190000	2M17	120AC	3000	3050	P6	95	10000	39000
8V13	120AC	5000	326250	P4	120	5000	3250	P37	95	5000	40000
8S1	110AC	7000	293250	Q28	120	5000	3250	P22	95	5000	51750
8T6	110AC	7000	366250	Q40	120AC	5000	3250	Q38	93	10000	53000
8V12	110AC	7000	624500	Q15	120	200	3314	P10	90	5000	69000
4S14	110AC	7000	654500	P5	120AC	5000	3500	Q12	90	5000	77000
8T7	110AC	7000	756500	P21	120AC	5000	3500	P15	90	10000	78000
				Q3	120AC	5000	3500	P8	89	5000	60000
				2M7	120AC	1000	3550	Q25	89	5000	67000
				2N2	120AC	1000	3750	1S14	85AC	5000	69750
				P20	120AC	5000	3750	V8	85	5000	71000
				Q36	120	200	4003	V26	85	5000	72000
				Q19	120AC	5000	6750	1T7	85AC	5000	81250
				2K22	120AC	5000	6750	Q32	85	5000	83000
				1V13	110	100	3610	Q14	85	5000	87000
				1T24	110AC	1000	5925	2M4	85	5000	89500
				1T29	110AC	1000	6100	T21	85	5000	94000
								1T5	85AC	5000	96000

^aMultiply by 6.8948 to convert to MN/m².

^bMultiply by 0.0167 to convert to Hz.

^cSpecimens with letter designations R, S, T, U, or V were from a different heat, and these data were used only in appendix C.

^dThe letters AC designate air-cooled specimen.

^eDesignates a runout; specimen did not fail after 10 million cycles.

TABLE III. - Concluded. ROTATING BENDING FATIGUE TEST DATA OBTAINED

AT CONSTANT NOMINAL STRESS AMPLITUDE

Specimen	Stress level	Test frequency, rpm	Cycles to failure	Specimen	Stress level	Test frequency, rpm	Cycles to failure
	(a), (d)	(b)			(a), (d)	(b)	
SAE 4130 (soft) steel; R. R. Moore machine				SAE 4130 (hard) steel; R. R. Moore machine			
P16	85	5000	97000	9E6	230AC	1000	200
2N5	85	5000	102250	9A5	220AC	1000	300
X26	95	5000	108000	9F17	220AC	1000	400
P33	85	5000	108000	9A12	200AC	1000	550
2N25	85	5000	112250	9D16	200AC	1000	575
V33	85	5000	129000	9C15	200AC	1000	650
V11	85	5000	133000	9F35	200AC	1000	650
2L9	85	5000	136000	9G26	200AC	100	681
2J39	35	5000	139000	9F1	200AC	1000	725
W33	85	5000	194000	9F6	200AC	1000	750
2K21	85	5000	210000	9B3	200AC	100	769
1V31	80AC	2000	91400	9B11	200AC	100	795
1U34	80AC	2000	110400	9E11	200AC	2500	800
016	80	10000	118000	9C22	175AC	1000	2870
1V30	80AC	2000	135725	9C25	175AC	1000	2900
1U20	80AC	2000	144025	9E33	175AC	1000	3120
2011	80AC	2000	147675	9F9	175AC	1000	3280
023	80	5000	160000	9E36	175AC	1000	3425
2K26	80	5000	168000	9F31	175AC	1000	3520
2N18	80AC	2000	169225	9B17	175AC	1000	3680
P9	80	5000	177000	9G3	150AC	1000	11525
2M18	80	5000	178000	9F16	150AC	1000	11625
P36	80	5000	184000	9F30	150AC	1000	12175
2N16	80AC	2000	187050	9B36	150AC	1000	12925
2M38	80	5000	204000	9F13	150AC	1000	13900
2M13	80	5000	218000	9331	150AC	1000	14000
1U11	80AC	2000	219325	9F4	150AC	1000	15000
2L32	80	5000	231000	9B35	150AC	1000	15525
2L16	80	5000	244000	9C39	100	3600	69250
2K38	80	5000	267000	9A27	100	1000	73600
2M5	80	5000	270000	9B29	100	1000	81500
2L26	80	5000	279000	9C8	100AC	5000	82250
2K6	80	5000	282000	9A37	100	3600	88250
2L18	80	5000	292000	9D28	100	3600	95750
2L30	80	5000	296000	9E21	100	1000	120500
2L19	80	5000	354000	9B34	100	1000	142300
2M26	75AC	5000	155750	9G24	100AC	5000	158500
1T1	75AC	5000	156750	9E3	100	1000	173025
1U3	75	100	157700	9B24	100	1000	253200
2N26	75AC	5000	171500	9F37	100	1000	481500
04	75	5000	173000				
1S38	75AC	5000	203000				
2025	75AC	5000	208500				
P14	75	5000	215000				
01	75	5000	223000				
1T35	75AC	5000	231500				
039	75	5000	252000				
031	75	5000	264000				
P19	75	5000	319000				
011	75	10000	355000				
034	75	5000	358000				
P34	75	5000	369000				
017	75	5000	548000				
013	75	5000	551000				

^aMultiply by 6.8948 to convert to MN/m².

^bMultiply by 0.0167 to convert to Hz.

^dThe letters AC designate air-cooled specimen.

TABLE IV. - AXIAL FATIGUE TEST DATA
 OBTAINED AT CONSTANT STRAIN
 AMPLITUDE WITH
 MARAGING STEEL

Specimen	Strain range, longitudinal total	Cycles to failure
V6	0.1361	30
V19	.0717	99
V59	.0717	110
V13	.0517	243
V15	.0517	283
V60	.0368	330
V62	.0368	474
V65	.0265	720
V4	.0264	848
V5	.0210	1 566
V20	.0170	3 170
V3	.0142	5 516
V14	.0135	8 234
V9	.0122	17 406
V67	.0115	15 780
V69	.0115	16 118
V22	.0112	17 775
V12	.0104	53 608
V25	.0097	156 630
V7	.0093	166 572
V26	.0092	338 140
V1	.0088	241 327

TABLE V. - ROTATING BENDING FATIGUE DATA OBTAINED IN TWO-STRESS-LEVEL TESTS

Specimen	First stress level, ksi (a)	First frequency, rpm (b)	Cycles applied, n ₁	Second stress level, ksi (a)	Second frequency, rpm (b)	Cycles to failure	Specimen	First stress level, ksi (a)	First frequency, rpm (b)	Cycles applied, n ₁	Second stress level, ksi (a)	Second frequency, rpm (b)	Cycles to failure
Maraging steel; Krouse machine							Maraging steel; Krouse machine						
8K9	270	100	200	240	100	2628	8B17	260	100	800	180	3000	7600
8B2	290	100	400	240	100	2008	8K1	260	100	1200	180	3000	4700
8H5	290	100	600	240	100	1444	8A7	260	100	1600	180	3000	3100
8H16	290	100	800	240	100	982	8E16	260	100	2000	180	3000	2300
8J17	290	100	1000	240	100	962	8N13	260	100	100	160	3000	35100
8L15	290	100	100	200	3000	9500	8M12	260	100	200	160	3000	24700
8N9	270	100	200	200	3000	8900	8L2	260	100	400	160	3000	23400
8P15	290	100	400	200	3000	5400	8P1	260	100	600	160	3000	16600
8P8	270	100	600	200	3000	4300	80--	260	100	1200	160	3000	6400
8L16	290	100	800	200	3000	3500	8N5	260	100	1800	160	3000	4300
8P17	290	100	1000	200	3000	2000	8P13	260	100	200	120	3000	172500
8E9	290	100	200	160	5000	25500	8P10	260	100	400	120	3000	97000
8C11	290	100	200	160	5000	17000	8L17	260	100	600	120	3000	53600
8F8	290	100	400	160	5000	17100	8Q2	260	100	1200	120	3000	20000
8K8	290	100	600	160	5000	9500	8N14	260	100	1400	120	3000	17300
8G15	290	100	800	160	5000	8600	8Q4	260	100	200	105	5000	1319200
8G8	270	100	1000	160	5000	3097	8P3	260	100	400	105	5000	415600
8G17	290	100	200	120	5000	125600	8Q16	260	100	600	105	5000	74100
8H6	290	100	200	120	5000	115700	8P12	260	100	1200	105	5000	40700
8G13	290	100	400	120	5000	54400	8N4	260	100	1800	105	5000	20100
8A6	270	100	600	120	5000	31800	8J9	240	3000	500	140	5000	45200
8E18	290	100	800	120	5000	21700	8Q3	240	3000	600	140	5000	56200
8C12	290	100	1000	120	5000	15700	8E6	240	3000	1000	140	5000	47000
8L9	290	100	100	105	5000	684700	8A18	240	3000	1000	140	5000	24700
8U9	290	100	200	105	5000	178500	8B7	240	100	1000	140	5000	24000
8L4	270	100	400	105	5000	80200	8G5	240	3000	1600	140	5000	14800
8N11	290	100	600	105	5000	84700	8C13	240	3000	2000	140	5000	18300
8P--	290	100	300	105	5000	29100	8A3	240	100	2000	140	5000	12800
8H9	270	100	100	170	5000	24900	8Q2	240	100	3000	140	5000	8600
8K12	270	100	200	170	5000	19300	8E2	240	3000	3100	140	5000	11800
8J10	270	100	400	170	5000	14000	8J5	240	3000	3200	140	5000	9300
8Q9	270	100	800	170	5000	8800	8A14	210	100	500	140	3000	100400
8B10	270	100	1200	170	5000	4600	8K10	210	3000	1000	140	3000	53900
8C18	270	100	1600	170	5000	1500	8C17	210	3000	2000	140	3000	30700
9L13	266	100	100	200	3000	11900	8Q6	210	3000	4000	140	3000	23400
8P4	266	100	300	200	3000	7700	8F15	210	3000	6000	140	3000	17200
8N2	266	100	600	200	3000	6200	8F2	210	3000	8000	140	3000	3000
8L5	266	100	1000	200	3000	4700	8P5	200	1000	1000	160	3000	40800
8M8	266	100	1500	200	3000	2600	8N10	200	1000	1000	160	3000	25000
8P14	266	100	100	105	5000	1094600	8N12	200	1000	2500	160	3000	34900
8M17	266	100	400	105	5000	180400	8Q5	200	1000	5000	160	3000	12500
8P9	266	100	600	105	5000	104200	8M7	200	1000	7500	160	3000	8600
8M4	266	100	1000	105	5000	51300	8L11	200	1000	10000	160	3000	8700
8L3	266	100	1500	105	5000	30100	8L7	200	1000	1000	120	5000	722400
8E12	260	100	100	180	3000	21300	8L6	200	1000	2500	120	5000	351400
8C8	260	100	200	180	3000	15800	8Q7	200	1000	3700	120	5000	47000
8H3	260	100	400	180	3000	10000	8N15	200	1000	5000	120	5000	79400
8D13	260	100	600	180	3000	12500	8Q12	200	1000	7500	120	5000	19100
							8M1	200	1000	10000	120	5000	8000

^aMultiply by 6.8948 to convert to MN/m².
^bMultiply by 0.0167 to convert to Hz.

TABLE V. - Continued. ROTATING BENDING FATIGUE DATA OBTAINED IN TWO-STRESS-LEVEL TESTS

Specimen	First stress level, ksi (a)	First frequency, rpm (b)	Cycles applied, n ₁	Second stress level, ksi (a)	Second frequency, rpm (b)	Cycles to failure	Specimen	First stress level, ksi (a), (e)	First frequency, rpm (b)	Cycles applied, n ₁	Second stress level, ksi (a), (e)	Second frequency, rpm (b)	Cycles to failure
Maraging steel - Krouse machine							Maraging steel - R. R. Moore machine						
8P2	160	3000	4000	120	5000	451900	883	300AC	100	25	130AC	5000	215000
8M16	160	3000	4000	120	5000	230500	8830	300AC	100	50	130AC	5000	97000
8L12	160	3000	17000	120	5000	50900	8C30	300AC	100	50	130AC	5000	98750
8N16	160	3000	16000	120	5000	34800	8C3	300AC	100	75	130AC	5000	126250
8L8	160	3000	24000	120	5000	22200	8A24	300AC	100	100	130AC	5000	74000
8Q8	160	3000	32000	120	5000	11100	8B40	300AC	100	100	130AC	5000	95500
8B12	240	100	750	290	100	123	8C7	300AC	100	100	130AC	5000	295000
8D5	240	100	1500	290	100	1058	8A13	300AC	100	150	130AC	5000	59750
8G9	240	100	2250	290	100	589	8C27	300	100	200	130	5000	48000
8J18	240	100	3000	290	100	342	8C29	300AC	100	200	130AC	5000	56250
8D17	160	3000	6000	290	100	1484	8C23	300AC	100	300	130AC	5000	41500
8A17	160	3000	17000	290	100	1178	8C14	300AC	100	500	130AC	5000	30500
8J13	160	3000	24000	290	100	1302	8A6	300AC	100	700	130AC	5000	16500
8D18	160	3000	36000	290	100	1388	8A21	190AC	1000	1000	130AC	5000	374250
8E17	160	3000	48000	290	100	33	8A14	190AC	1000	2000	130AC	5000	94000
8J1	140	5000	20000	240	3000	4000	8C20	190AC	1000	4000	130AC	5000	46500
8H1	140	5000	20000	240	3000	3700	8C28	190AC	1000	7000	130AC	5000	26000
8J16	140	5000	40000	240	3000	4300	8A18	190AC	1000	10000	130AC	5000	19500
8H10	140	5000	40000	240	3000	3300	8A26	160AC	1000	4000	130AC	5000	486000
8D14	140	5000	60000	240	3000	4500	888	160AC	1000	9000	130AC	5000	454250
8D12	140	5000	60000	240	3000	4300	8C8	160AC	1000	17000	130AC	5000	182250
8C16	140	5000	70000	240	3000	c c	8A27	160AC	1000	16000	130AC	5000	93750
8A12	140	5000	80000	240	3000	2900	8822	160AC	1000	32000	130AC	5000	30000
8F17	140	5000	80000	240	3000	c c	8324	130AC	5000	100000	300AC	100	946
8C14	120	5000	50000	290	100	1145	8C19	130AC	5000	200000	300AC	100	1009
8H18	120	5000	100000	290	100	1103	8A32	130AC	5000	300000	300AC	100	989
8A15	120	5000	150000	290	100	1209	886	130AC	5000	350000	300AC	100	c c
8H11	120	5000	200000	290	100	1230	8C9	130AC	5000	400000	300AC	100	905
							882	130AC	5000	450000	300AC	100	c c
							8C1	130AC	5000	450000	300AC	100	1131
							8T16	190AC	100	500	110AC	7000	389000
							8S2	130AC	100	1000	110AC	7000	161500
							8S6	190AC	100	2000	110AC	7000	86000
							8V5	190AC	100	4000	110AC	7000	34500
							8V4	190AC	100	6000	110AC	7000	18750

^aMultiply by 6.8948 to convert to MN/m².

^bMultiply by 0.0167 to convert to Hz.

^cSpecimen failed at first stress level.

^dSpecimens with letter designations R, S, T, U, or V were from a different heat, and these data were used only in appendix C and fig. 14.

^eThe letters AC designate air-cooled specimen.

TABLE V. - Concluded. ROTATING BENDING FATIGUE DATA OBTAINED IN TWO-STRESS-LEVEL TESTS

Specimen	First stress level, ksi (a), (e)	First frequency, rpm (b)	Cycle applied, n ₁	Second stress level, ksi (a), (e)	Second frequency, rpm (b)	Cycles to failure	Specimen	First stress level, ksi (a), (e)	First frequency, rpm (b)	Cycle applied, n ₁	Second stress level, ksi (a), (e)	Second frequency, rpm (b)	Cycles to failure
SAE 4130 (soft) steel - R. R. Moore machine							SAE 4130 (soft) steel - R. R. Moore machine						
1T25	140AC	100	50	120AC	100	1449	1S6	100AC	2000	8000	85AC	3000	22500
1S34	140AC	100	100	120AC	100	1148	1T10	100AC	2000	12000	85AC	3000	11750
1T36	140AC	100	200	120AC	100	886	1S7	100AC	2000	1000	75AC	5000	147250
1T38	140AC	100	300	120AC	100	730	1T6	100AC	2000	2000	75AC	5000	152750
1S24	140AC	100	400	120AC	100	304	2016	100AC	2000	2000	75AC	5000	148000
1S26	140AC	100	25	100AC	3000	8750	1S23	100AC	2000	4000	75AC	5000	47000
1S35	140AC	100	50	100AC	5000	4500	1S14	100AC	2000	5000	75AC	5000	53750
1S13	140AC	100	50	100AC	5000	4000	2012	100AC	2000	5000	75AC	5000	141500
1T30	140AC	100	100	100AC	5000	4000	1S1	100AC	2000	8000	75AC	5000	47250
1S36	140AC	100	200	100AC	2000	2500	1T24	100AC	2000	12000	75AC	5000	22750
1S17	140AC	100	300	100AC	2000	1850	SAE 4130 (hard) steel; R. R. Moore machine						
1T22	140AC	100	25	85AC	3000	43700	9F26	200AC	100	100	100AC	5000	59750
1T34	140AC	100	50	85AC	3000	27925	9013	200AC	100	200	100AC	5000	30000
1T2	140AC	100	100	85AC	3000	19400	9G27	200AC	100	400	100AC	5000	14000
1S37	140AC	100	200	85AC	3000	8000	9F33	200AC	100	600	100AC	5000	8500
1T8	140AC	100	300	85AC	3000	6000							
2N31	140AC	100	25	75AC	5000	123000							
1T20	140AC	100	50	75AC	5000	79000							
2020	140AC	100	100	75AC	5000	59000							
2013	140AC	100	200	75AC	5000	39750							
2020	140AC	100	300	75AC	5000	32000							
1V36	140AC	100	400	75AC	5000	12750							
1T26	140AC	100	500	75AC	5000	4750							
1S9	120AC	100	100	110AC	1000	4700							
1S31	120AC	100	200	110AC	1000	3125							
1T28	120AC	100	500	110AC	1000	2825							
1S22	120AC	100	1000	110AC	1000	1300							
1S29	120AC	100	1500	110AC	1000	250							
1T31	120AC	100	100	100AC	3000	13000							
1S15	120AC	100	200	100AC	3000	6500							
1T19	120AC	100	500	100AC	3000	4250							
1S25	120AC	100	1000	100AC	3000	2250							
2N32	120AC	100	1000	100AC	3000	4750							
1V16	120AC	100	1500	100AC	3000	1500							
1T9	120AC	100	100	85AC	5000	47250							
1S20	120AC	100	200	85AC	5000	28500							
1T4	120AC	100	500	85AC	5000	19250							
1S5	120AC	100	1000	85AC	5000	6500							
1T39	120AC	100	1500	85AC	5000	3000							
206	120AC	100	200	75AC	5000	86000							
2J36	120AC	100	500	75AC	5000	44000							
1T3	120AC	100	1000	75AC	5000	27250							
2035	120AC	100	1500	75AC	5000	26000							
2N21	120AC	100	2000	75AC	5000	11000							
1S12	100AC	2000	1000	85AC	3000	68250							
1T21	100AC	2000	2000	85AC	3000	46500							
1T37	100AC	2000	4000	85AC	3000	45750							
1S27	100AC	2000	6000	85AC	3000	32750							

^aMultiply by 6.8948 to convert to MN/m².

^bMultiply by 0.0167 to convert to Hz.

^cThe letters AC designate air-cooled specimen.

TABLE VI. - AXIAL FATIGUE DATA OBTAINED IN TWO-STRAIN-LEVEL

TESTS OF MARAGING STEEL

Specimen	First strain level	Cycles applied, n	Second strain level	Cycles to failure
V53	0.0368	10	0.0115	14 866
V50	↓	20	↓	10 400
V49	↓	60	↓	6 060
V74	↓	100	↓	2 708
V75	↓	100	↓	3 205
V47	↓	100	↓	5 720
V48	↓	200	↓	3 365
V51	↓	300	↓	1 965
V54	.0717	20	.0265	532
V63	↓	40	↓	440
V56	↓	60	↓	435
V52	↓	75	↓	285
V55	.0717	20	.0368	364
V57	↓	40	↓	284
V58	↓	60	↓	168
V64	↓	80	↓	180
V66	.0115	4 000	.0368	444
V72	↓	8 000	↓	15
V73	↓	8 000	↓	230
V70	↓	12 000	↓	116

TABLE VII. - SUMMARY OF ROTATING BENDING FATIGUE DATA OBTAINED IN
TWO-STRESS-LEVEL ALTERNATING BLOCK TESTS WITH MARAGING STEEL

[Test conditions: initial stress, σ_1 , 190 000 psi (1310 MN/m²); second stress, σ_2 , 110 000 psi (758 MN/m²); cycles to failure at initial stress, $N_{f,1}$, 8000 cycles; cycles to failure at second stress, $N_{f,2}$, 625 000 cycles; cycles of Phase I at initial stress, $N_{o,1}$, 1300 cycles.]

Specimen	Cycle ratio, $n/N_{o,1}$	Cycles applied per block		Summation of cycles applied at initial stress, $\sum n_1$	Summation of cycles applied at second stress, $\sum n_2$	Cycle ratio summation, $\sum \frac{n}{N_f}$
		At initial stress, n_1	At second stress, n_2			
8R1	0.22	285	19 750	1995	126 250	0.45
8U13	.22	285	19 750	2280	147 750	.52
8V14	.22	285	19 750	3135	204 000	.72
8U7	.29	380	26 250	1900	118 250	.43
8R12	.29	380	26 250	1900	127 000	.44
8T14	.29	380	26 250	2739	183 750	.64
8U3	.44	570	39 250	1140	77 250	.27
8R5	.44	570	39 250	2850	193 000	.66
8S12	.44	570	39 250	3420	224 500	.79
8R4	.55	710	49 000	2130	129 750	.47
8T5	.55	710	49 000	2130	134 750	.48
8U9	.55	710	49 000	3550	208 750	.78
8U2	.65	850	58 750	1700	97 500	.37
8U5	.65	850	58 750	3400	225 500	.79
8T2	.65	850	58 750	4250	241 750	.92
8R11	.76	990	68 500	1980	134 250	.46
8U6	.76	990	68 500	2970	151 000	.62
8T1	.76	990	68 500	3960	257 500	.91
8R8	.87	1130	78 500	2260	90 000	.43
8R9	.87	1130	78 500	2260	139 000	.51
8V1	.87	1130	78 500	3390	178 000	.71
8U4	.87	1130	78 500	5650	325 000	1.23
8S15	.99	1280	87 500	1280	70 500	.27
8S3	.99	1280	87 500	2560	128 500	.53
8T13	.99	1280	87 500	2560	150 000	.56

"The aeronautical and space activities of the United States shall be conducted so as to contribute . . . to the expansion of human knowledge of phenomena in the atmosphere and space. The Administration shall provide for the widest practicable and appropriate dissemination of information concerning its activities and the results thereof."

—NATIONAL AERONAUTICS AND SPACE ACT OF 1958

NASA SCIENTIFIC AND TECHNICAL PUBLICATIONS

TECHNICAL REPORTS: Scientific and technical information considered important, complete, and a lasting contribution to existing knowledge.

TECHNICAL NOTES: Information less broad in scope but nevertheless of importance as a contribution to existing knowledge.

TECHNICAL MEMORANDUMS: Information receiving limited distribution because of preliminary data, security classification, or other reasons.

CONTRACTOR REPORTS: Scientific and technical information generated under a NASA contract or grant and considered an important contribution to existing knowledge.

TECHNICAL TRANSLATIONS: Information published in a foreign language considered to merit NASA distribution in English.

SPECIAL PUBLICATIONS: Information derived from or of value to NASA activities. Publications include conference proceedings, monographs, data compilations, handbooks, sourcebooks, and special bibliographies.

TECHNOLOGY UTILIZATION PUBLICATIONS: Information on technology used by NASA that may be of particular interest in commercial and other non-aerospace applications. Publications include Tech Briefs, Technology Utilization Reports and Notes, and Technology Surveys.

Details on the availability of these publications may be obtained from:

SCIENTIFIC AND TECHNICAL INFORMATION DIVISION
NATIONAL AERONAUTICS AND SPACE ADMINISTRATION

Washington, D.C. 20546